Roses produce the floral scent compound 2-phenylethanol via a new biosynthetic pathway in response to seasonal change in environment

THESIS

Roses produce the floral scent compound 2-phenylethanol *via* a new biosynthetic pathway in response to seasonal change in environment

Hiroshi Hirata

Graduate School of
Science and Technology, Educational Division
Department of Bioscience
Shizuoka University

January 2012

THESIS

Roses produce the floral scent compound 2-phenylethanol *via* a new biosynthetic pathway in response to seasonal change in environment

（バラ香気成分2－フェニルエタノールの季節性環境変化に応答した新規生合成経路）

平　田　　拓

静岡大学

大学院自然科学系教育部

バイオサイエンス専攻

２０１２年１月

Contents

General Introduction

General Introduction

Floral scent compounds

Plants synthesize and release a large variety of volatile organic compounds, which can be considered as the plant's interface with the surrounding[1,2]. These volatile compounds are released from flowers, leaves, fruits, and roots into the atmosphere or soil, allowing the plant to interact with other organisms while remaining anchored to the ground. Floral scent compounds serve as attractants for species-specific pollinators, bees and moths, and have an important role in the reproductive processes[3,4]. Therefore emission of floral scent compounds are synchronizes with activity of pollinators to exhibit diurnal or nocturnal rhythmic emission[5]. They also have a considerable economic value in guaranteeing yield and quality of many crops, and enhance the aesthetic properties of ornamental flowers.

Volatiles are low molecular weight metabolites (less than 300 Da) with diverse chemical structures (hydrocarbons, alcohols, aldehydes, ketones, ethers, and esters), and originate from several biosynthetic pathways, including the terpenoid, phenylpropanoid / benzenoid, and lipoxygenase pathways. In general, the scent of flowers are composed of complex mixtures of tens or sometimes hundreds of volatile compounds arising from diverse biochemical pathways.

1) Terpenoids: Many terpenoids, *e.g.* hemiterpenes (C5), monoterpenes (C10), sesquiterpenes (C15), homoterpenes (C11 and C16), and some diterpenes (C20) have a high vapor pressure allowing their release into the atmosphere. The building blocks of all terpenoids are the universal five carbon precursors, isopentenyl diphosphate (IPP) and its allelic isomer dimethylallyl diphosphate (DMAPP).

2) Phenylpropanoids and Benzenoids: Phenylpropanoids and benzenoids constitute the second most ubiquitous class of plant volatile compounds and are derived from the amino acid L-phenylalanine (L-Phe). Despite their abundance, diversity, and importance in the scent and aroma of countless plant species, the precise biochemical pathways leading to the formation of volatile phenylpropanoids and their derivatives are still mostly unknown.

3) Fatty Acid and Amino Acid Derivatives: Volatile fatty acid derivatives such as *cis* -3-hexenol, 1-hexanal, nonanal, and methyl jasmonate constitute another important group of plant volatiles which are present in the scent and aroma of numerous

flowers and fruits. These compounds originate from C18 unsaturated fatty acids (linoleic or linolenic acids), which enter the "lipoxygenase pathway".

Thus floral volatiles are diversified but it is generally believed that similar biosynthetic reactions may occur in flowers although not all the corresponding enzymes have been identified yet.

2-Phenylethanol in rose and its physiological role in plant

2-Phenylethanol (2PE) is one of the prominent scent compounds produced by Damask roses such as *R*osa *x damascena*, *R.* 'Hoh-Jun', and *R.* 'Yves Piaget' (Figure 1), and in various fruits such as strawberry, tomato and grape varieties[6]. 2PE and phenylacetaldehyde (PAld), a precursor of 2PE, characterize flavors in wine and cheese[7]. These compounds associate with pleasant sweet flowery notes at low concentration and the world's annual production of 2PE was estimated to be approximately 10,000 tons in 2010[8,9]. The amounts of these compounds emitted are dependent on environmental photoperiod. As the activity of the pollinators is synchronized with the photoperiod, the emission of volatile compounds is at peak when the pollinators are active[5,10]. Diurnal rhythmic emission patterns of 2PE, benzyl alcohol, monoterpene alcohols, and monoterpene hydrocarbons were observed in *R. damascena semperflorens* '*Quatra Saisons*'[11]. The similar rhythmic emission was observed even in rose cultivars developed for ornamental use (*e.g.*, *R.* 'Hoh-Jun)[12] or cut flowers (*e.g.*, *R.* 'Yves Piaget').

There are a few reports on the physiological roles of 2PE and related compounds, although they are likely to be involved in attracting pollinators. PAld is reported to function as a kairomone in *Cirsium arvense*[13]. 2PE plays a role in attracting the thrips in the family Annonaceae, *Xylopia aromatica*[14]. Therefore 2PE should play a crucial role of reproductive process in flower. There is considerable interest in elucidating the biosynthetic pathways of 2PE, especially in rose flowers where it is a predominant volatile. We have investigated the volatiles and its biosynthesis, since the biosynthesis of floral volatiles will provide 'More fragrant flower' as plant engineering.

Rosa damascena Mill.

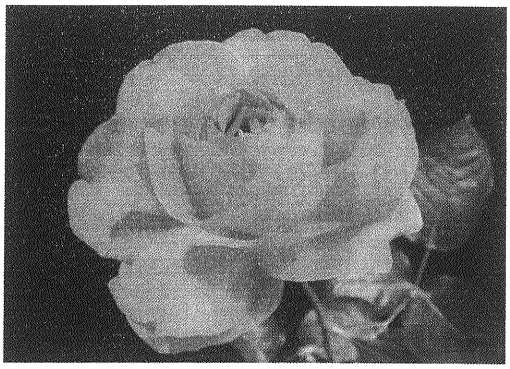

Rosa 'Yves Piaget'

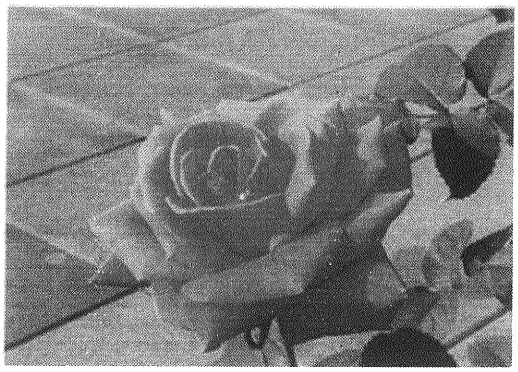

Rosa 'Hoh-Jun'

Figure 1. Photo of *Rosa* damascena Mill., *R.* 'Hoh-Jun' and *R.* 'Yves Piaget.'

Biosynthesis of 2-phenylethanol

To investigate 2PE biosynthesis, we have traced the number of ^2H isotope as a chemical prove. In *R. damascena* and *R.* 'Hoh-Jun' deuterium labeled 2PE as a dominant isotopomer was detected with feeding L-[$^2H_8$]Phe to intact rose flowers, suggesting that [$^2H_8$]-2PE was derived from L-[$^2H_8$]Phe with retention of the α-position deuterium atom[12]. This feeding experiment of deuterium labeled compound proposed a biotransformation pathway for 2PE production *via* several intermediates including 2-phenylethylamine, phenylacetaldoxime and phenylacetaldehyde (PAld) (Figure 2)[15]. To confirm 2PE biosynthetic pathway, pyridoxal-5'-phosphate (PLP)-dependent aromatic amino acid decarboxylases (AADC) and phenylacetaldehyde reductases (PAR), 2PE biosynthesis *via* PAld in roses, were characterized biochemically[16]. AADC transformed L-Phe to PAld *via* the Schiff base, which was formed by a reaction between the amino group of L-Phe and a formyl group on PLP. PAld was also synthesized by Plant PAld synthase (PAAS) in *Petunia hybrida*[17] and AADC in *Solanum lycopersicum*[18]. The PAld was converted to 2PE by the action of PAR[19,20]. Thus, [$^2H_8$]-2PE was synthesized from L-[$^2H_8$]Phe *via* [$^2H_8$]-PAld by the action of both enzymes, AADC (PAAS) and PAR, in plants.

Recently we have established protoplasts systems as an experimental model of 2PE biosynthesis[21]. Rose protoplasts produced [^2H_n, n=6-8]-2PE from L-[$^2H_8$]Phe as well as intact rose flowers. However, over a couple of years in Shizuoka, Japan, we conducted L-[$^2H_8$]Phe feeding experiments with protoplasts made from flowers of *R.* 'Yves Piaget' and [$^2H_7$]-2PE as a main isotopologue was synthesized by the protoplasts around summer seasons (about July-September) in both years. In contrast, [$^2H_8$]-2PE was synthesized as the main product around winter seasons (about December-February)[21]. As referred above by the number of deuterium of 2PE suggested its synthesis pathway[12]. Therefore we hypothesized that rose flowers produced [$^2H_7$]-2PE *via* different pathway from AADC-PAR pathway. This study is focusing on the biosynthesis of 2PE isotopologues and the 'seasonal change' of 2PE biosynthesis.

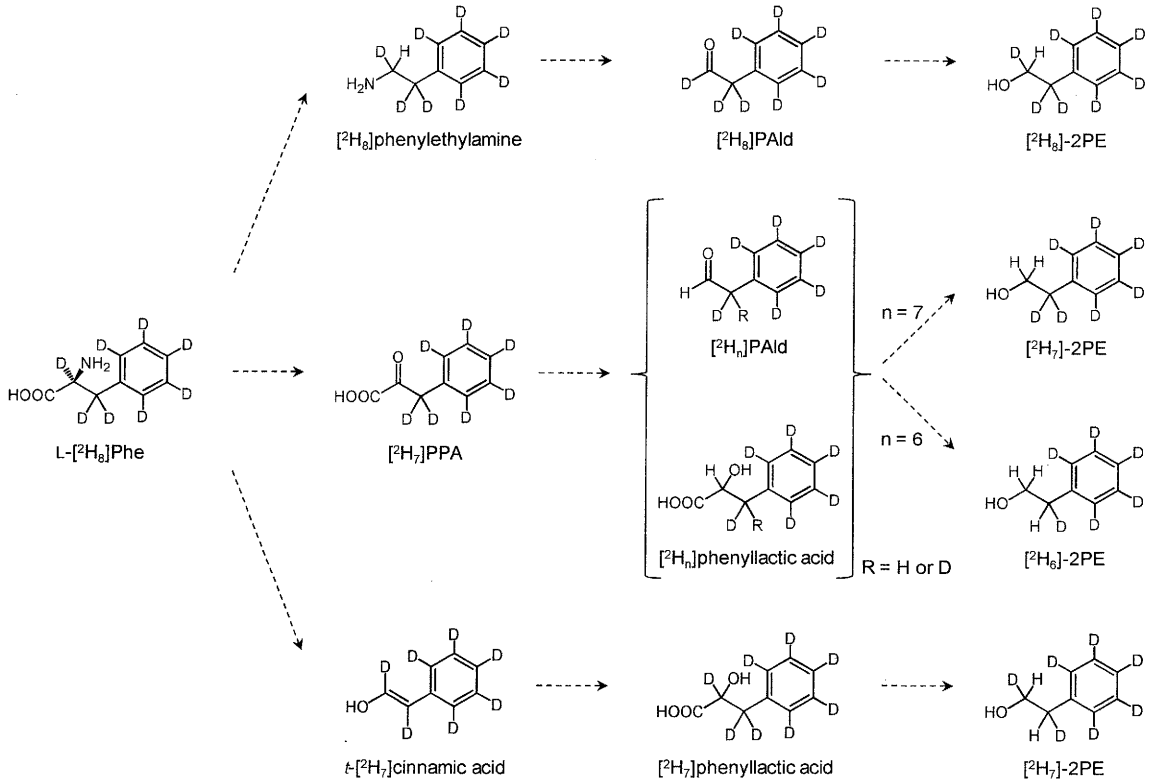

Figure 2. Hypothetical biogenetic pathway for [^2H_n, n=6-8]-2PE from L-[^2H_n]Phe.

Chapter 1

Seasonal changes of production in [$^{2}H_{n}$, n=6–8]-2PE isotopologues and hypothetical intermediate, phenylpyruvic acid in rose protoplasts

I-1. Introduction

2PE is produced from L-Phe without loss of α-hydrogen of it, resulting in [$^2H_8$]-2PE production upon L-[$^2H_8$]Phe feeding to intact flower. GC-MS analysis revealed that [$^2H_7$]-2PE as a main isotopologue was synthesized by the protoplasts around summer in both years. To investigate the hypothesis to produce [$^2H_7$]-2PE *via* different biosynthetic pathway in response to surroundings, we further investigated [$^2H_7$]-2PE production in rose flower protoplasts system.

I-2. Material and methods

I-2-1. Plant materials, preparation of protoplasts, and protoplast treatments

Cut flowers of *Rosa* 'Yves Piaget' were purchased from Ichikawa Rosary in Mishima-City, Shizuoka prefecture, Japan. The stages of floral growth have been described previously[12]. Protoplasts were prepared as described previously[21]. L-[$^2H_8$]Phe and PPA were dissolved in protoplast buffer and added to the protoplasts at final concentrations of 2.5 μmol. The protoplasts were incubated at 30 °C for 24 hours and then ethyl decanoate in methanol (1.55 nmol) was added as an internal standard. The volatiles were extracted twice with 700 μl of hexane:ethyl acetate (1:1 v/v). The organic fraction was dried over Na_2SO_4 and subjected to GC-MS analyses.

I-2-2. Chemicals and biochemicals

L-[2,3,3,2',2,'4',5',6'-$^2H_8$]Phe (98 atom% ^2H, Aldrich) was used in the pulse chase studies. The ratio of L-[2,3,3,2',2,'4',5',6'-$^2H_8$]Phe ([$^2H_8$]L-Phe)/L-[3,3,2',2,'4',5',6'-$^2H_7$]Phe ([$^2H_7$]L-Phe)/ [$^2H_6$]L-Phe is estimated to be 83/16.5/0.5 based on the ^1H-NMR analyses as previously reported[12]. [$^2H_8$]-/[$^2H_7$]-/[$^2H_6$]-2PE = 83/16.5/0.5 should be produced when any ^2H atoms were not be abstracted or replaced with protons during the pulse-chase feeding experiments. The production ratio of [$^2H_8$]-/[$^2H_7$]-/[$^2H_6$]-2PE was determined based on the ion intensities at *m/z* 130, *m/z* 129, and *m/z* 128 for molecular ions of [$^2H_8$]-, [$^2H_7$]-, and [$^2H_6$]-2PE, respectively. An abstraction of a ^2H atom at C3 (benzyl) position yielded a decline in the ion intensity at *m/z* 98 [$C_6{}^2H_7$]$^+$, the ion intensity at *m/z* 98, *m/z* 97, and *m/z* 96 were used to confirm the chemical structure of [$^2H_8$]-2PE and [$^2H_7$]-2PE. All the other chemicals were of the highest grade commercially available, unless noted otherwise.

I-2-3. Analysis of 2-phenylethanol and phenylacetaldehyde by GC-MS

Analyses of 2PE, [^2H_n, n=6–8]-2PE, and PAld were performed using a GC-MS QP5050 (Shimadzu), which was controlled by a Class-5000 work station. For the analyses of 2PE and [^2H_n, n=6–8]-2PE, the GC was equipped with a capillary TC-WAX column (GL Sciences Inc., Japan) of 30 m × 0.25 mm I.D. and 0.25 μm film thickness. The column temperature was elevated from 60 °C (3 min hold) to 180 °C (40 °C /min) then to 240 °C (10 °C/min, 3 min hold). The injector temperature was 200 °C, the ionizing voltage was 70 eV, and the scanning speed was 0.5 scen/s with a *m/z* range of 76–200. For PAld analysis, the GC was equipped with a capillary TC-5 column (30 m × 0.25 mm I.D., 0.25 μm film thickness, GL Sciences Inc., Japan). the column temperature was elevated from 50 °C (3 min hold) to 90 °C (10 °C/min), then to 130 °C (30 °C/min) and then 290 °C (40 °C/min, 3 min hold). The injector temperature, the ionizing voltage, the scanning speed, and the *m/z* range were same condition with 2PE analysis.

I-2-4. Determination of phenylpyruvic acid and [^2H_n, n=6-7] phenylpyruvic acid by LC-MS

In order to measure the production of [$^2H_7$]-PPA, protoplasts were administered with L-[$^2H_8$]Phe (24 h at 30 °C) and then lyophilized. The powders were dissolved in 15 ml Milli-Q water and applied to an SPE cartridge (Supelclean™ ENVI-Chrom P SPE Tube, 500 mg). The eluate was concentrated and redissolved in 100 μl 5% MeCN. The LC-MS separation module was equipped with a SHIMADZU SPD-M10A DAD, LC-MS2010A, and the separation was performed on a YMC-Pack ODS AQ column (2.0×150 mm, YMC) connected to a GUARD CARTRIDGE CAPCELL C18 UG120 (4.0×10 mm, SHISEIDO). The solvents used were A: 5 mM ammonium acetate (pH 7.0), and B: MeCN[24]. The gradient was developed by increasing the latter from 5% to 90% in 13.5 min, then holding the concentration constant for 2.5 min with a flow rate of 0.2 ml/min at 40 °C. The PPA detection range was 90 to 370 nm and the MS detection system was operated in the negative ionization mode with a scan range of *m/z* 100–300. The tuning parameters were as follows: capillary voltage 3.5 kV; cone voltage 20 V; source block temperature 120 °C; and desolvation temperature 350 °C. The mass range scanned was 50 to 1,500 D at a 2 sec. scan rate. The PPA and [$^2H_7$]-PPA retention times were 6.71 and 6.66 min, respectively.

I-2-5. Preparation of crude enzymes from the flowers of *R.* 'Yves Piaget'

The rose petals were crushed in liquid nitrogen, and lyophilized to obtain powdered material. For the L-Phe conversion, this material (0.7 g) was homogenized in 0.1 M Tris-HCl buffer pH 8.0 containing 0.1 mM PLP, 1 mM EDTA, 1% glycerol and 0.1% TritonX-100 in the presence of 5.3 g PVPP (Polyclar 10, ISP Japan). After centrifugation (26,000 *g*, 15 min, 4 °C), the supernatant was precipitated with ammonium sulfate (0-80%). Then additional centrifugation (26,000 *g*, 30 min, 4 °C) gave the pellets, and it was dissolved in Tris-HCl buffer pH 8.0 containing 0.1 mM PLP, 1 mM EDTA and 1% glycerol and supplied to transaminase assay with L-Phe as the substrates and α-keto-glutalic acid, described in below. For the PPA conversion, the powdered material (1.0 g) was homogenized in 0.1 M citrate buffer pH 6.0 containing 1% TritonX-100 in the presence of 5.7 g PVPP. After centrifugation (26,000 *g*, 15 min, 4 °C), 100 μL the supernatant and 50 mM PPA (2.5 μmol) in a 0.1 M citrate buffer pH 6.0 were incubated at 35 °C for 2 h and then ethyldecanoate in methanol (1.55 nmol) was added as an internal standard. The volatiles were extracted with 400 μL of hexane:ethyl acetate (1:1, v/v). The organic fraction was dried over Na_2SO_4 and subjected to GC-MS analyses. GC-MS conditions were described below.

I-2-6. Assay of L-phenylalanine transamination activity

Reaction mixtures (150 μL) containing 10 mM L-Phe, 10 mM α-keto-glutaric acid and 30 μL enzyme solution in a 0.5 M Tris-HCl buffer (pH 9.0) were incubated at 45 °C for 10 min. The reaction was stopped by adding equal volumes MeCN and 200 nmol L-[$^2H_8$]Phe as an internal standard. After centrifugation (20,000 *g*, 10 min, 4 °C), the sample was filtered (Millex LH, Millipore) and analyzed by LC-MS.

I-2-7. Assay of phenylpyruvic acid decarboxylation activity

Reaction mixtures (200 μL) containing 5 mM PPA, 0.1 mM Thiamine pyrophosphate, 0.5 mM $MgCl_2$ and 100 μL enzyme solution in a 0.1 M citrate buffer (pH 6.0) were incubated at 35 °C for 2 h. The reaction was stopped by adding 400 μl hexane : ethylacetate (1:1, v/v) and 23.3 pmol 3-phenylpropion aldehyde as an internal standard. After centrifugation (20,000 *g*, 1 min, 4 °C), the organic phase was anhydrous and then analyzed by GC-MS.

I-3. Results

I-3-1. Seasonal variation of [^2H_n, n=6–8]-2-phenylethanol isotopologues as a main products

Rose protoplasts were prepared from rose petals and fed with L-[$^2H_8$]Phe. We found that [$^2H_7$]-2PE (*m/z* 129 $[M]^+$) as the main product ([$^2H_8$]/[$^2H_7$]/[$^2H_6$]-2PE=9.8/76.4/13.9) was detected in the protoplasts collected in summer (August, 2008) whereas [$^2H_8$]-2PE (*m/z* 130 $[M]^+$) became the dominant product ([$^2H_8$]/[$^2H_7$]/[$^2H_6$]-2PE=75.6/21.0/3.4) in winter (January, 2009) (Figure 1-1 *A* and *B*). Based on the results, [$^2H_7$]-2PE was dominantly produced with a loss of ^2H at α-position (C-2) of L-[$^2H_8$]Phe in summer season, suggesting the presence of an alternative biosynthetic pathway of 2PE around summer season. Thus we hypothesized that the novel 2PE biosynthetic pathway includes the intermediate phenylpyruvate (PPA) and two key enzymes: AAAT and KDC (Fig. 1-2).

I-3-2. Monitoring of [^2H_n, n=6–8]-2-phenylethanol production in rose protoplasts

To verify the seasonal variation in the synthesis of 2PE, L-[$^2H_8$]Phe was administered to the floral protoplasts harvested once every month from May 2009 to July 2010. [$^2H_7$]-2PE was the dominant species detected among the [^2H_n, n=6–8]-2PE isotopologues from May to October although low levels of [$^2H_8$]-2PE were also detected (Fig. 1-1 *C* and *D*). In contrast, [$^2H_8$]-2PE was the dominant compound detected from November to April. Thus, [$^2H_8$]-2PE was synthesized constantly throughout the year and [$^2H_7$]-2PE was synthesized with 5–10 fold higher than the [$^2H_8$]-2PE from May to October.

I-3-3. Transformation of L-[$^2H_8$]phenylalanine to [^2H_n, n=6-7] phenylpyruvic acid in rose protoplasts

To confirm the involvement of PPA in the new 2PE biosynthetic pathway, we analyzed L-[$^2H_8$]Phe transformation to [$^2H_7$]-PPA, a key intermediate in the new pathway, in rose protoplasts harvested in the period from May to October. [$^2H_7$]-PPA (*m/z* 170 [M-H]) was detected at a retention time (7.05 min) that coincided with that of authentic PPA (Figure 1-3), together with ion peaks of *m/z* 168 (44%) [[$^2H_5$]-PPA-H]$^-$, *m/z* 169 (39%) [[$^2H_6$]-PPA-H]$^-$ and *m/z* 170 (16%) [[$^2H_7$]-PPA-H]$^-$, suggesting a replacement of ^2H atoms in [$^2H_7$]-PPA due to keto-enol tautomerism[25,26]. These results

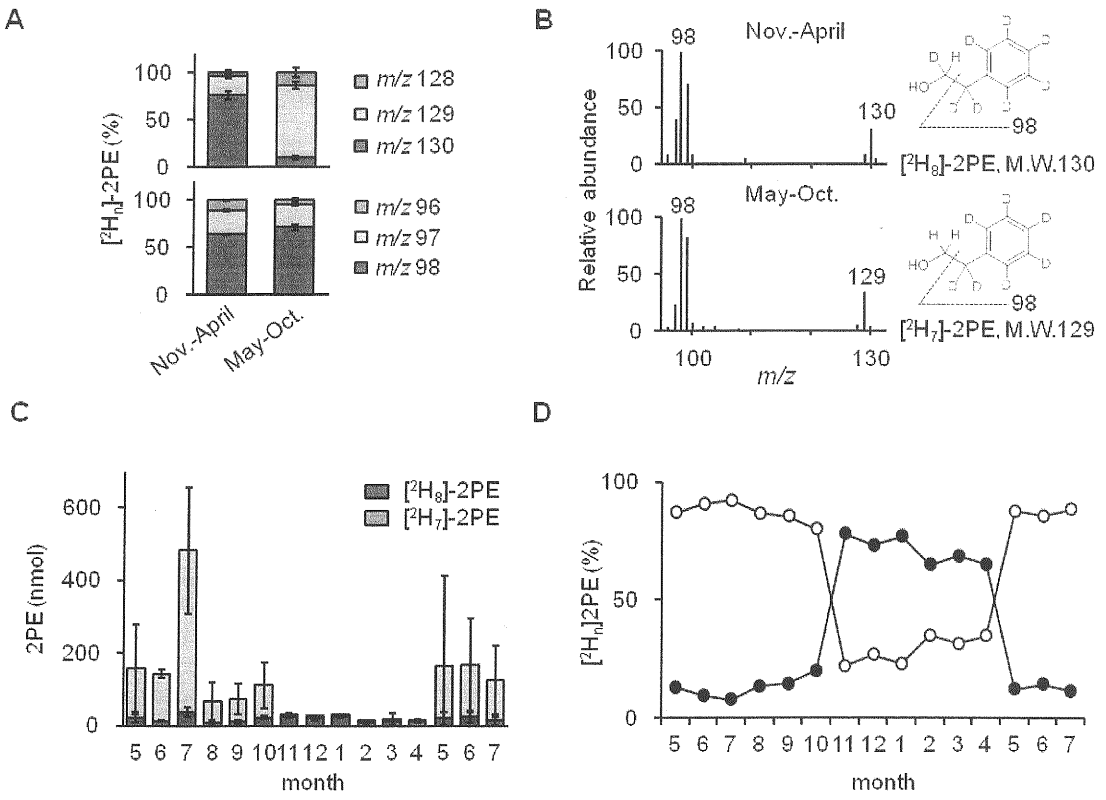

Figure 1-1. Synthesis of [^2H_n, n=6–8]-2PE and hypothetical biosynthetic pathway to 2PE. (A) Ratio of synthesized [^2H_n, n=6–8]-2PE in protoplasts collected between May and October and between November and April. Molecular ions and benzyl cations are shown in the upper and lower diagrams, respectively. (B) Mass spectra of the [^2H_n, n=6–8]-2PE that were produced in November to April (upper) and in May to October (lower). Monthly changes of [$^2H_8$]- and [$^2H_7$]-2PE in the amounts (C) and ratio (D) produced throughout the year.

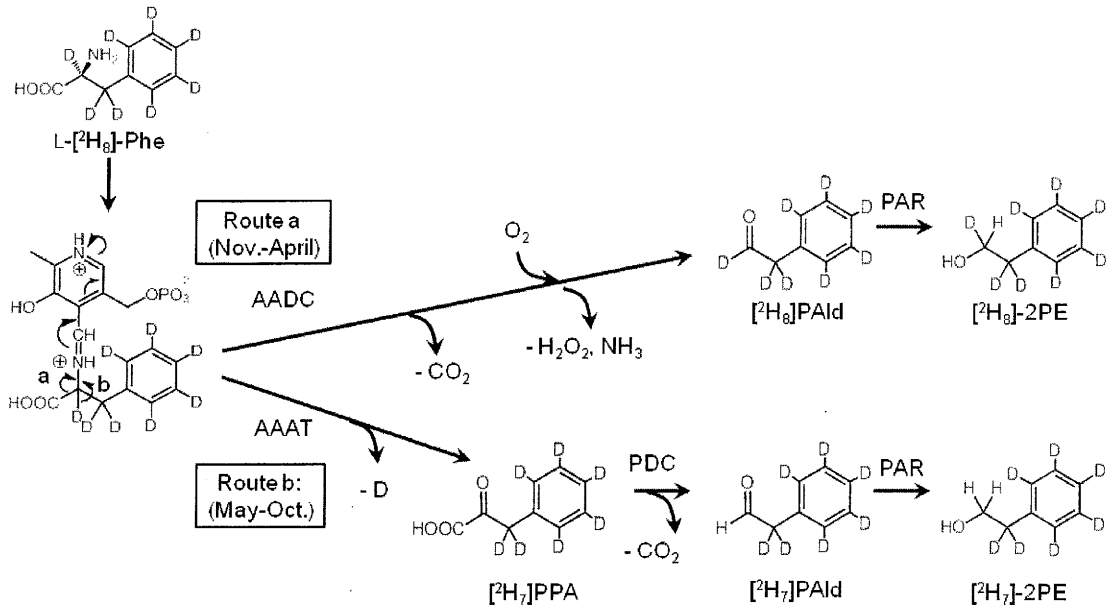

Figure 1-2. Proposed reaction mechanisms resulting in the different labeling of [$^2H_8$]-2PE and [$^2H_7$]-2PE synthesized from L-[$^2H_8$]Phe in rose petals. [$^2H_8$]-PAld is synthesized by AADC after Schiff base formation and release of carbon dioxide, with retention of the α-deuterium of L-[$^2H_8$]Phe (Route a). In contrast, PDC forms a Schiff base and releases the α-deuterium prior to decarboxylation, to yield [$^2H_7$]-PAld (Route b). In both routes, [^2H_n, n=7, 8]-PAld is converted to 2PE by PAR.

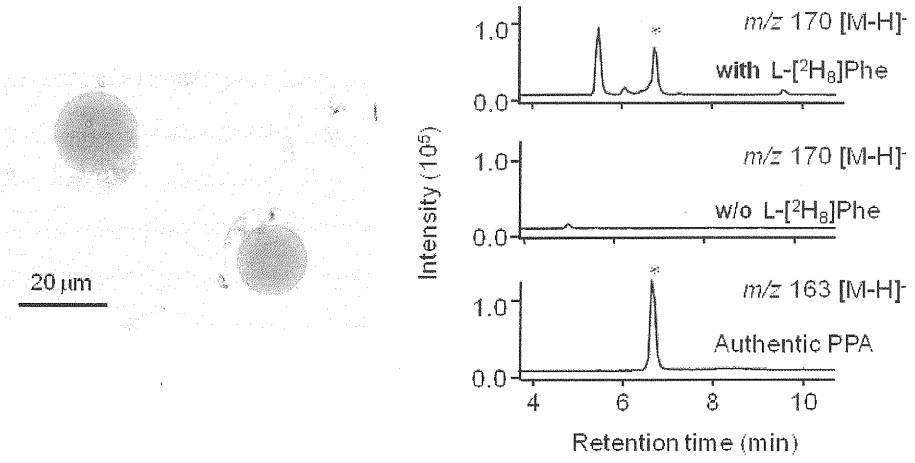

Figure 1-3. Determination of [$^2H_7$]PPA production in rose protoplasts. Typical rose petal protoplasts (Left). The scale bar indicates 20 μm. LC-MS chromatogram of [$^2H_7$]PPA in protoplasts (Right). [$^2H_7$]PPA (*m/z* 170 [M-H]$^-$, with asterisk) was detected at a retention time (6.66 min), which was identical to that of authentic PPA (asterisk, *m/z* 163 [M-H]$^-$). [$^2H_7$]PPA was not detected in the protoplasts without (w/o) L-[$^2H_8$]Phe feeding.

showed that PPA was a key intermediate, and strongly suggested that AAAT catalyzed the transformation of L-[$^2H_8$]Phe to [$^2H_7$]-PPA.

I-3-4. Enzymatic conversion of two reactions in the new 2-phenylethanol biosynthesis

We also determined the transamination activity from L-Phe to PPA and conversion from PPA to PAld in the crude enzymes prepared from rose petals. PPA was detected by LC-MS based on the detection of peaks of the trace at *m/z* 163 $[M-H]^-$ with the same retention time of authentic PPA (Figure 1-4*A*), revealing that L-Phe was converted to PPA by the enzymes in the *R.* 'Yves Piaget'. Furthermore, we detected PAld production in crude enzymatic assay mixture with PPA as a substrate by GC-MS (Figure 1-4*B*), revealing that PPA was converted to PAld, precursor of 2PE. Together these results demonstrated that PPA is a biosynthetic intermediate in the new 2PE biosynthetic pathway in rose flowers.

I-3-5. Comparison of transformation activity of rose protoplasts in different seasons

To confirm the transformation of PPA to 2PE, we administered either L-[$^2H_8$]Phe or PPA to rose protoplasts harvested from May to October, and from November to April. Each compound was transformed to [^2H_n, n=6-8]-2PE and 2PE, respectively (Figure 1-5). When L-[$^2H_8$]Phe or PPA was administered, the production of [^2H_n, n=6-8]-2PE or 2PE was much higher in the May–October samples than in the November–April samples ($P < 0.01$). These results suggested that 2PE was produced from PPA *via* PAld and the biosynthetic route is activated in the period from May to October.

I-4. Discussion

Microorganisms biosynthesized 2PE from L-Phe *via* PPA, called 'Ehrlich pathway'[22], while there is no reports about Ehrlich pathway in *planta* so far. In microorganism, the amino acids metabolism has been studied in detail and aminotransferases play a critical role in forming the corresponding keto-acids that serve as substrates for multiple biochemical reactions[23]. Furthermore, the new pathway of 2PE in rose seemed to be activated in May-October than in November-April. Here, meteorological parameter, temperature and vapor pressure drew in seasonal shape at

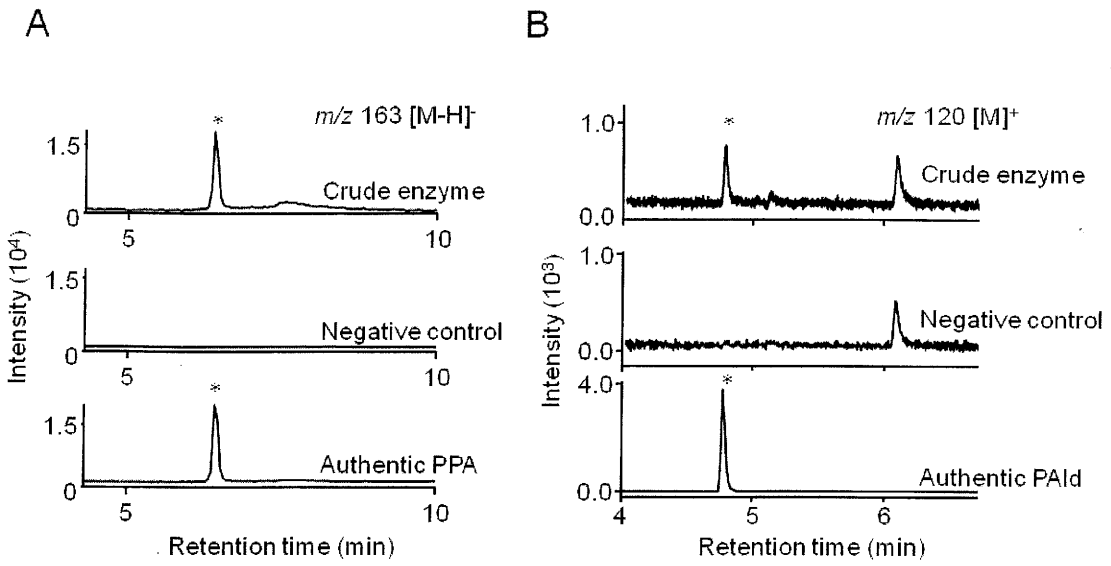

Figure 1-4. Conversion of L-Phe to PPA and PPA to PAld with a crude enzyme. (A) LC-MS chromatogram of L-Phe conversion to PPA. (B) GC-MS chromatogram of PPA conversion to PAld. PPA (retention time = 6.66 min) was traced at *m/z* 163 $[M-H]^-$ on LC-MS, and PAld (retention time = 4.56 min) was traced at *m/z* 120 $[M]^+$ by GC-MS. The asterisks indicated peaks of PPA (A) and PAld (B), respectively. The PAld production from PPA increased time-dependently in the presence of the crude enzyme. Negative control stands for the chromatograms of the reaction mixtures at the beginning of the enzymatic reaction. PAld production from PPA by chemical conversion was negligible during the incubation period.

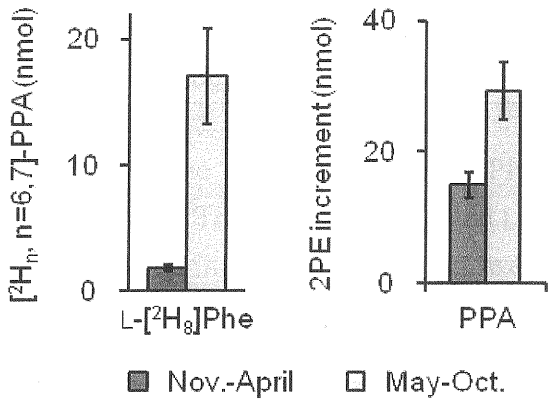

Figure 1-5. Transformation activity in both seasons of L-[$^2H_8$]Phe and PPA. Comparison of PPA and 2PE synthetic activities in the protoplasts collected between May and October and between November and April. The activities are evaluated as the [^2H_n, n=6-7]PPA production and increments of 2PE, respectively.

Mishima-city where rose flowers grown was varied with the seasons (Figure 1-6). It is possible that the seasonal variation in 2PE biosynthesis might be one of an adaptation to the climate change. Although it is not unclear that 2PE synthesis is activated by an environmental factor, these results suggested that rose flowers have two different pathways and the seasonal production of [$^2H_7$]-2PE might response to an environmental change.

We demonstrated the alternative route converted L-Phe to PPA and then PPA to PAld with crude enzymes from rose petals. These results indicated L-Phe was converted to PAld *via* PPA with enzymatical reaction in rose flowers. Also, we were successful to detect [$^2H_7$]PPA in rose petal protoplasts with feeding L-[$^2H_8$]Phe, suggesting the transamination of L-Phe to PPA working *in vivo*, but we could not detect endogenous PPA in rose petal protoplasts by LC-MS. Similarly the endogenous PPA was not determined in petunia but upon feeding shikimic acid PPA was firstly measureable[27]. These suggested that PPA would be pretty quickly converted to PAld in plant. Our conversion study here strongly suggested that 2PE is biosynthesized from L-Phe *via* PPA in rose flowers and rose AAAT forms PPA enzymatically from L-Phe. Therefore we supposed PPA is presumably converted by a decarboxylase to PAld in the second step of new 2PE biosynthetic pathway.

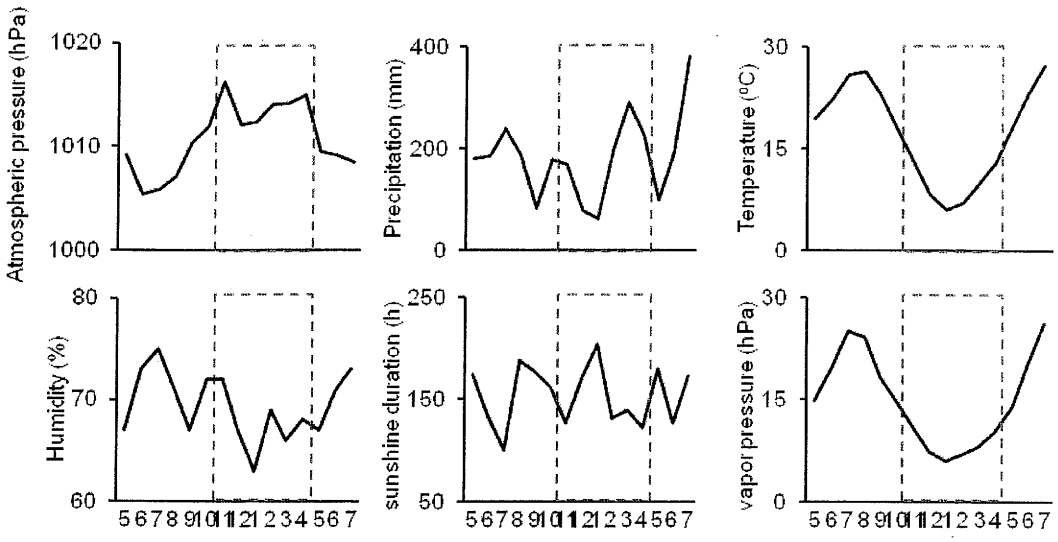

Figure 1-6. Meteorological parameter in Mishima-city. Dashed red square shows during the period of November-April, corresponding to $[^2H_n]$-2PE production as a main isotopologue. All data sets were obtained from Mishima Local Meteorological Observatory.

Chapter 2

Determination of Aromatic amino acid aminotransferase producing phenylpyruvic acid from rose petals

II-1. Introduction

PPA production was detected in protoplasts and cell-free extracts from rose flowers, and [$^2H_7$]PPA was highly produced in May-October samples than in November-April samples. Thus we supposed AAAT contributes to production of [$^2H_7$]-2PE in summer season as well as Ehrlich pathway. Therefore we next tried to identify rose AAAT producing PPA from L-Phe.

II-2. Material and methods

II-2-1. EST database of rose flowers

R. 'Hoh-Jun' petals (stage 5, 5 g) were supplied to RNA extraction with RNeasy Plant Mini Kit (QIAGEN) and then purified to obtain mRNA with Oligotex-dT30 mRNA Purification Kit (TaKaRa). EST database was constructed by Dragon genomyx center (TaKaRa Bio, Japan).

II-2-2. Molecular cloning of RyAAATs and expression in *E. coli.*

Degenerate RyAAATs primers (Appendix Table 2-1) were designed using conserved regions among aspartate aminotransferases (AspATs) (GenBank association numbers: NP001031394, NP850022, NP565529, AAQ54557, BAD54126, BAD27593, BAD19094, NP178152, NP177890, NP001118421, and NP180654), and the tyrosine aminotransferase (TyrAT) EST (CF349437 in *R.* hybrid cultivar)[28] and the alanine aminotransferase (AlaAT) (in-house rose EST database). These cDNAs of RyAAAT candidates were amplified by RT-PCR from total RNA extracted from stage 3 rose petals. The PCR products were cloned into the pCR2.1 TA-Cloning vector (Invitrogen) and sequenced, and then 3 different sequences of RyAAAT candidates were subcloned into the pET28a expression vector, which contains an N-terminal histidine tag (Novagen). The cloned genes were expressed in *E. coli* BL21(DE3) cells grown in LB medium with 50 μg/mL kanamycin at 37 °C. Protein production was induced by the addition of 1 mM IPTG (TaKaRa). After incubation at 27 °C for 24 h, the crude proteins were extracted with 20 mM potassium phosphate buffer (pH 7.5) containing 0.75 mM PLP and 0.1% Triton X-100 (Extraction buffer). The proteins were purified with HisTrap HP column (GE Healthcare) equilibrated with the Extraction buffer (without Triton X-100) and eluted using a linear 0–0.75 M imidazole gradient in the same buffer.

Protein concentrations were determined using Bradford reagents (Bio-Rad) with bovine serum albumin as the standard.

II-2-3. RyAAAT3 substrate specificity

The substrate specificity for transamination of RyAAAT3 was determined by quantification of the various keto-acid products. The reaction was initiated by the addition of the amino acid and performed at 45 °C under V_{max} conditions for L-Phe. The reaction was stopped by adding equal volumes MeCN and 200 nmol L-[$^2H_8$]Phe as an internal standard. After centrifugation (20,000 *g*, 10 min, 4 °C), the sample was filtered (Millex LH, Millipore) and then analyzed by LC-MS (L, D-Phe, L-tyrosine, L-tryptophan) and an amino acid analyzer (Hitachi) (L-alanine and glycine). The products, PPA, 4-hydroxyphenylpyruvic acid and indole-3-pyruvic acid, were coincided with each authentic compound. As determined L-alanine and glycine decrease in amino acid analyzer, we followed manufacturing methods.

II-2-4.Inhibition of PLP-dependent enzymes with Carbidopa

We have reported rose AADC expression in *E. coli*[10]. The crude proteins were extracted with 20 mM potassium phosphate buffer (pH 7.5) containing 1 mM PLP and 0.1% CHAPS. The proteins were purified as described in RyAAATs expression. AADC assay mixtures (400 μL) containing 4 mM L-Phe and 200 μL enzyme solution in a 0.2 M potassium phosphate buffer (pH 8.0) were incubated at 35 °C for 1 h, and then PAld was extracted and analyzed described above. Inhibition assays of AADC and AAAT with Carbidopa[29,30] were performed as decarboxylation and transamination assay with or without carbidopa dissolved in 5% dimethylsulfoxide (DMSO) (final concentration).

II-2-5. Transcription analysis of *RyAAAT3*

Total RNA was extracted from various tissues derived from three different plants of *R.* 'Yves Piaget' at stage 4. RT-PCR was performed using primer sets for *RyAAAT3* and 18S *rRNA* (Ambion) as a house keeping gene. Competitor primers for 18S *rRNA* were used to avoid excess amplification of the 18S *rRNA*. The ratio of 18S *rRNA* primers and competitor primers was 4:6 (v/v). The transcripts were visualized on a 1% agarose gel stained with ethidium bromide and the amplification curves were at linear process as confirmed at various cycles. *RyAAAT3* primers are listed in Appendix Table

2-1.

II-2-6. RNAi suppression experiments

Two kinds of double strand RNA (dsRNA) were prepared based on *RyAAAT3* partial sequences. The dsRNA of RyAAAT3 were synthesized using the T7 RiboMAX System (Promega) and specific primers (Appendix Table 2-1), and annealed by incubation at 70 °C for 10 min[31,32]. The rose protoplasts (3×10^5 cells in 200 μL protoplast buffer) were transfected with 75 μg dsRNA using an equal volumes 40% polyethylene glycol-calcium solution (PEG 6000, Fluka)[33]. After incubation for 24 h at 30 °C, 2.5 μmol L-Phe was added to the protoplasts and they were incubated for another 24 h at 30 °C. 2PE extraction and GC-MS analysis was carried out as described above. Effect of Ry*AAAT3* knockdown was confirmed by RT-PCR as described above.

II-3. Results

II-3-1. Cloning and heterogeneous expression of RyAAATs

Blast searching and degenerate PCR cloning from rose petals gave us three EST candidates of RyAAAT catalyzing transamination of L-Phe and we obtained three independent full length cDNAs with 3', 5'-RACE cloning PCR and expressed in *E. coli* respectively (RyAAAT1, RyAAAT2 and RyAAAT3). We purified the expressed enzymes and evaluated the activity based upon PPA production. One of candidates (RyAAAT3), homologous to TyrAT, showed PPA production activity with L-Phe (Figure 2-1, 2-2). However other two RyAAAT1, 2 homologous with AspAT and AlaAT hardly showed any PPA production (Figure 2-3). RyAAAT3 is a 421 amino acid protein with a calculated average molecular weight of 46326 Da and pI of 6.28 (GenBank/EMBL accession number AB669189), and includes a aminotransferases family-I PLP attachment site (SLSKrwLVpGWRLG) and the highly conserved residue in family I for the binding of these enzymes substrates, arginine 393[34,35]. The deduced amino acid sequences of RyAAAT3 showed 78% similarity to *C. melo* AAAT. Based upon *in silico* analysis, TargetP 1.1 (http://www.cbs.dtu.dk/services/TargetP/), ChroloP 1.1 (http://www.cbs.dtu.dk/services/ChloroP/), SignalP 4.0 (http://www.cbs.dtu.dk/services/SignalP/) and WoLF PSORT (http://wolfpsort.org/), showed that RyAAAT3 does not contain signal peptides at its N terminal, suggesting cytosolic localization.

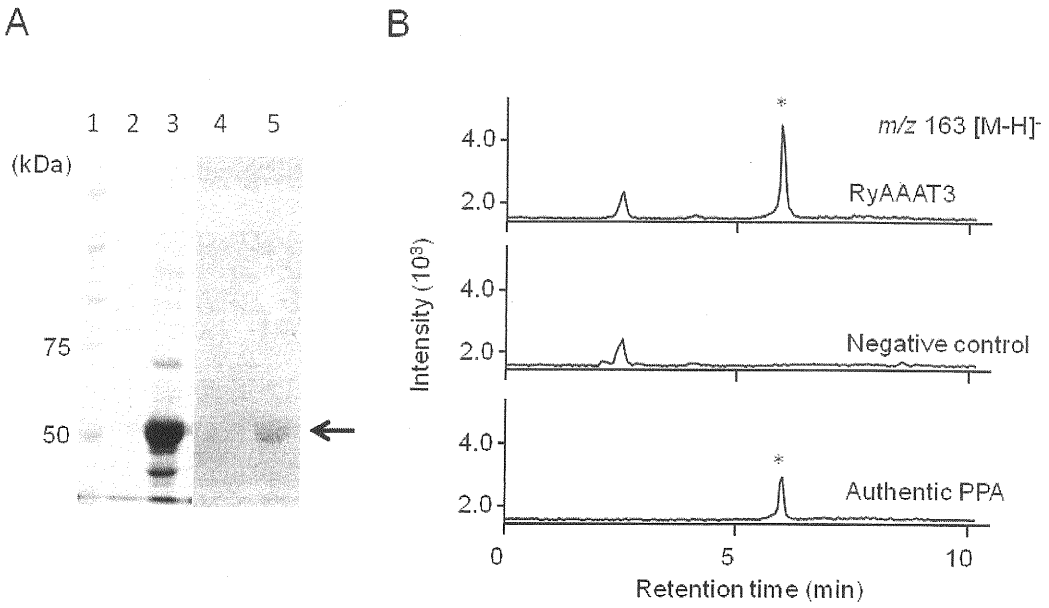

Figure 2-1. Heterogeneous expression and transaminase activity of RyAAAT3. (A) SDS-PAGE (lanes 1-5) of samples used in the RyAAAT3 activity analysis. Lane1-3 were stained CBB and lane 4, 5 were stained His-Detect In-Gel Stain (Nacalai Tesque). Lane 1, protein molecular markers; lanes 2 and 4, proteins expressed with empty vector; lanes 3 and 5, purified recombinant RyAAAT3 protein (arrow). (B) LC-MS chromatogram of enzymatic product of RyAAAT3. PPA (asterisks) was detected at 6.66 min on the LC-MS chromatogram monitored at *m/z* 163 $[M-H]^-$. Negative control on Fig. 3B indicates a LC-MS chromatogram monitored at *m/z* 163 $[M-H]^-$ for the reaction mixture at beginning of the reaction in the presence of L-Phe and RyAAAT3.

Figure 2-2. Amino acid sequence multiple alignments of RyAAAT3 and plant AAAT/TyrAT. *Cucumis melo* L. AAAT (CmAAAT, ADC45389), *Papaver somniferum* TyrAT (PsTAT, ADC33123), *Solanum pennellii* TyrAT 1 (SpTAT, ADZ24702) and *Arabidopsis thaliana* TyrAt (AtTAT, NP_200208). Black arrowheads indicate the conserved Lys residues that covalently bind the PLP cofactor and white arrowheads indicate conserved amino acids proposed to possess crucial roles in catalysis[35,36]. Underline shows aminotransferases family-I PLP attachment site. Black dots indicate *N*-glycosylation site predicted in Genetyx version 8.0 software.

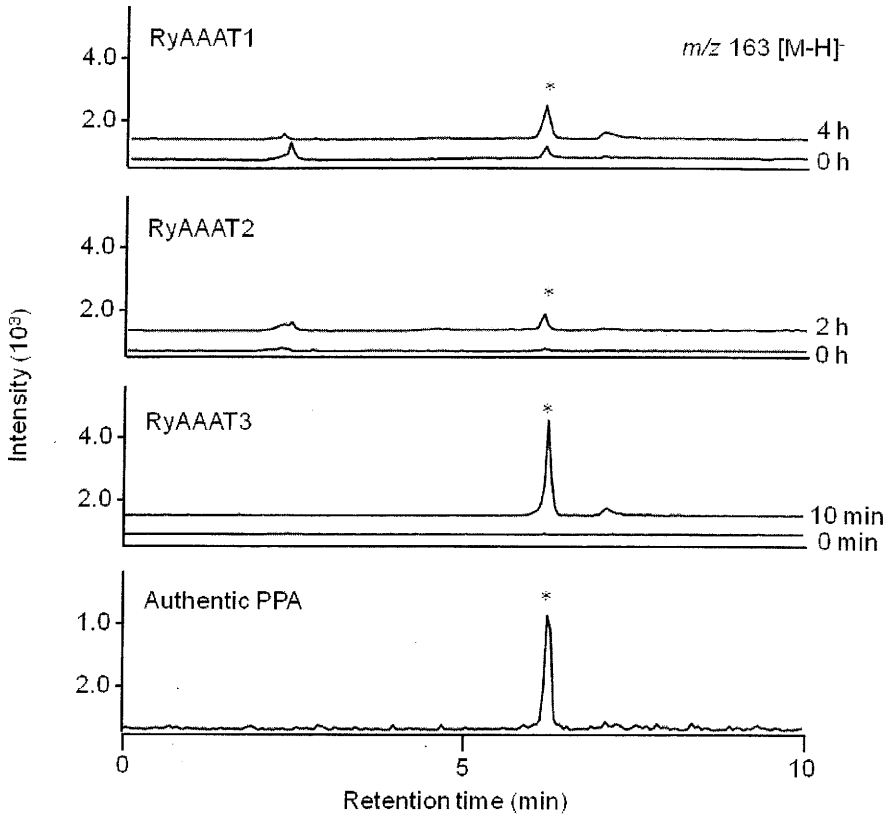

Figure 2-3. Comparison of transaminase activity among RyAAAT1-3. Total ion traces on LC-MS analyses of L-Phe metabolites produced with recombinant RyAAAT1-3 extracted from *E. coli* cultures. The asterisk depicts peak for authentic PPA and PPA detected in each chromatogram. PPA production did not detect in RyAAAT1 and 2 reaction mixture for 10 min reaction time.

II-3-2. Kinetic analysis of RyAAAT3 in transaminase reaction

Optimum pH of enzyme was screened in a range of 7-10 by monitoring the production of PPA (Figure 2-4A). Also, the optimum temperature for the PPA production was determined and the highest at 45 °C was observed (Figure 2-4B). In RyAAAT3, α-keto-glutaric acid was the preferred amino acceptor rather than oxalo acetic acid in production of PPA from L-Phe under the optimum conditions in pH and reaction temperature (Figure 2-5A). Recombinant RyAAAT3 revealed the K_m and V_{max} values for the conversion of L-Phe with oxalo acetic acid were 0.73 ± 0.11 mM, 6.86 ± 0.04 nmol/mg protein/min, respectively, and with α-keto-glutalic acid were 1.47 ± 0.37 mM, 21.85 ± 0.59 nmol/mg protein/min respectively (means ± SD; n=4).

II-3-3. Relative activity and direction of transaminase reaction

To further characterize the enzymatic properties of RyAAAT3, we analyzed relative activity of transamination with several amino acids such as L-Phe, D-phenylalanine, L-tyrosine and L-tryptophan. L-Phe gave the highest transaminase activity, on the other hand L-tyrosine and L-tryptophan aromatic amino acids gave one-quarter activity in comparison to L-Phe. This enzyme hardly showed any activity for substrates L-alanine, D-phenylalanine or glycine respectively (Figure 2-5B).

Aminotransferases catalyze *bi*-directional reactions in transamination. It proposes that L-Phe would be produced from PPA by aminotransferase in plants[37]. We also determined the reaction selectivity of RyAAAT3 in transamination. Forward reaction (L-Phe as a substrate, α-keto-glutalic acid as an amino acceptor) and the reverse reaction (PPA as a substrate, L-glutamic acid as an amino donor) were evaluated by LC-MS analyses for the products. The RyAAAT3 showed 9.7 fold higher transamination activity from L-Phe to PPA (19.37 ± 0.67 pmol/mg protein/min) than reverse reaction (2.01 ± 0.47 pmol/mg protein/min). These results suggested that RyAAAT3 preferred L-Phe as a substrate compared to PPA.

II-3-4. Inhibition of transamination by Carbidopa

It is well known that aminotransferase forms Schiff base between the amino group of amino acid residue of aminotransferase and PLP. Also, rose AADC was reported to produce PAld with forming Schiff base. To confirm whether RyAAAT3 is PLP dependent enzyme or not, we quantified the production of PAld and PPA in AADC (decarboxylation) and AAAT (transamination) enzymatic assays with Carbidopa.

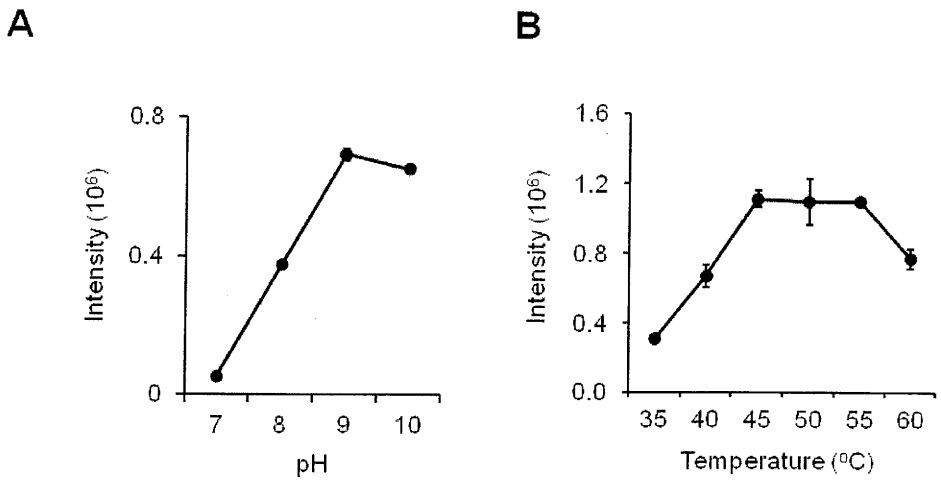

Figure 2-4. Characterization of RyAAAT3 enzymatical parameter. (A) Optimum pH; (B) optimum temperature in transaminase reaction producing PPA from L-Phe with α-keto-glutaric acid as an amino acceptor. (mean of 3 replicates ± SD).

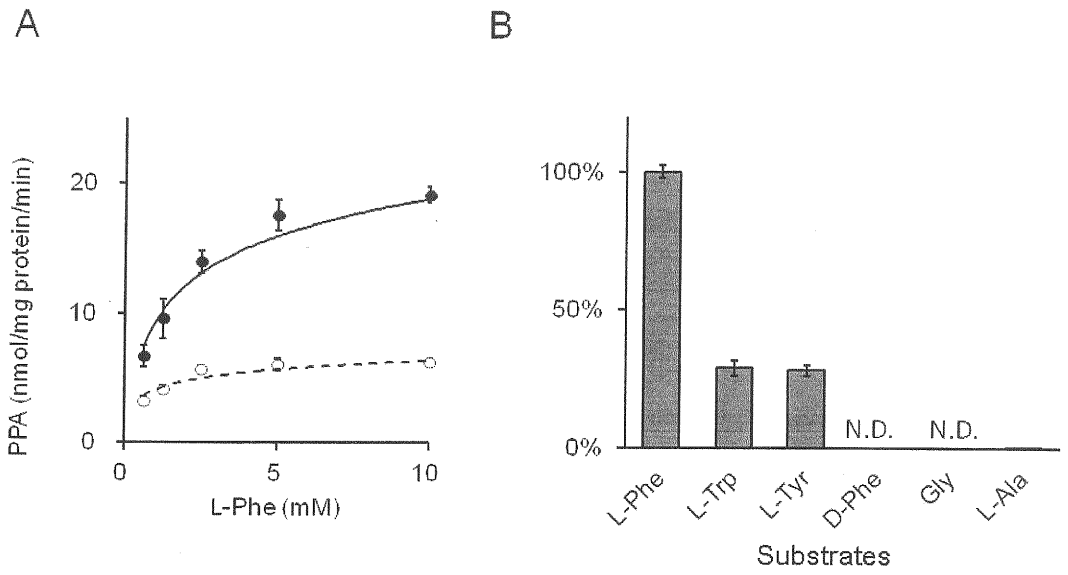

Figure 2-5. Characterization of RyAAAT3 in amino acceptor preference and substrate specificity. (A) RyAAAT3 kinetics with oxalo acetic acid (open circle) or α-keto-glutaric acid (closed circle). (B) Relative conversion of selected amino acids to their keto-acids, catalyzed by RyAAAT3. (Abbreviations are as follows: L-Phe; L-Phenylalanine, L-Trp, L-Tryptophan; L-Tyr, L-Tyrosine; D-Phe; D-Phenylalanine, Gly; Glycine, L-Ala; L-Alanine). Relative activities were determined under L-Phe V_{max} conditions. The activity (21.85 ± 0.59 nmol/mg protein/min) with L-Phe was taken at 100%. Amino acids were used at equal concentrations of 10 mM. N.D. means not detected. Error bars represent standard deviation (SD, n=3).

Carbidopa inhibited production of PAld and PPA with concentration dependent manner and at 500 μM concentration PAld and PPA were hardly produced in the heterogeneously expressed rose AADC and RyAAAT3 (Figure 2-6).
RyAAAT3 preferred L-Phe as a substrate compared to PPA.

II-3-5. Transcripts analysis of *RyAAAT3* in rose tissues

We examined transcription level of *RyAAAT3* in rose various tissues at stage 4 rose plants by RT-PCR. Total RNA was extracted from tissues of 3 independent of *R.* 'Yves Piaget' plants (harvested in September). *RyAAAT3* was expressed in rose petals and also other tissues, leaf, stem, rose hip and calyx (Figure 2-7). The *C. melo AAAT* was expressed at the same level in various organs, shoots, young and old leaves, and in immature fruits[38]. Also, PAAS in petunia and AADC in tomato expressed in various organs other than petals. The RyAAAT3 expressed in the petals should produce PPA from L-Phe in rose petals.

II-3-6. RNA interference of *RyAAAT3*

To elucidate the contributions of *RyAAAT3* to 2PE synthesis in the rose flowers, we performed RNAi experiments targeting *RyAAAT3* in the rose protoplasts. 2PE production in non-treated samples was almost the same compared to control samples. RNAi experiments towards *RyAAAT3* decreased 2PE production at about 60% as compared with the control samples (Figure 2-8). These results suggested *RyAAAT3* plays an important role in 2PE biosynthesis of in rose flowers.

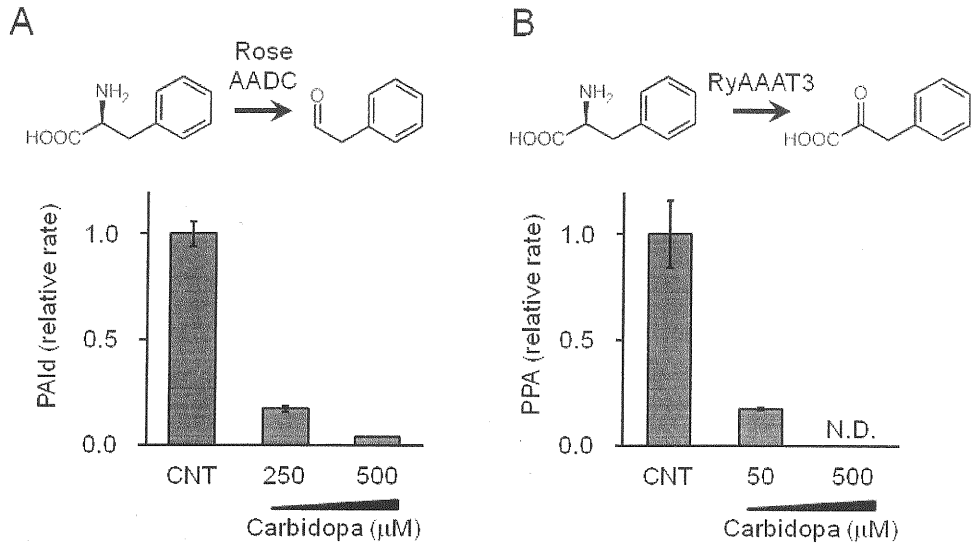

Figure 2-6. Inhibition of PLP-dependent enzymes, rose AADC and RyAAAT3. PAld (A) and PPA (B) productions were examined in the presence of Carbidopa based on the GC-MS and LC-MS, respectively. The amounts of PAld and PPA in the absence of Carbidopa were taken as 1.0 for CNT, a control group. N.D. means not detected. The relative rates were calculated based on the averages of three replicates ± SD.

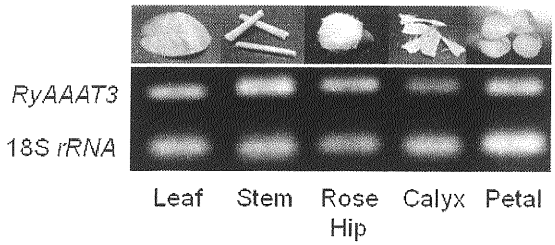

Figure 2-7. Transcriptional analysis of *RyAAAT3* in various organs of *R.* 'Yves Piaget'. Total RNA was extracted from tissues of 3 independent of *R.* 'Yves Piaget' plants (harvested in September). RT-PCR of 18S ribosomal RNA was used as a house keeping gene. *RyAAAT3* primers for transcriptional analysis are listed in Appendix Table 1.

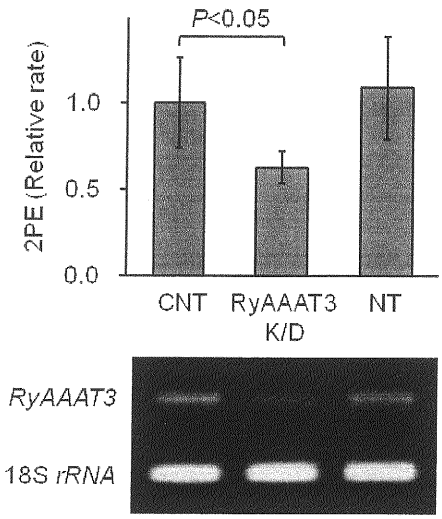

Figure 2-8. Effect of RNAi-mediated silencing of *RyAAAT3* in protoplasts. The 2PE synthesis was measured in protoplasts prepared from rose petals. The control (CNT) and knockdown groups (RyAAAT3 K/D) were treated with PEG-Ca solution, and the NT groups were not treated. Statistics analysis was performed in student *t*-test. The amount (15 nmol/10^5 protoplast cells) of 2PE production for CNT was taken as 1.0. The relative rates were calculated based on the averages of 2PE amounts in the CNT group and the data were obtained from each of three independent biological replicates ± SD.

II-4. DISCUSSION

Phenylalanine aminotransferases (PheATs) are classified in AAAT family, similarly TyrATs and tryptophan aminotransferases (TrpATs) and several research concerning enzymatic characterizations of AAATs have been reported[38-43]. Arabidopsis *WEAK ETHYLENE INSENSITIVE8* (*WEI8*) gene family link the tissue-specific effects of ethylene and auxin production[44] and the shade avoidance response of plants to low red/far-red light is essential for the expression of *SHADE AVOIDANCE3* (*SAV3*) gene[40]. These two genes, *WEI8* and *SAV3*, encode a TrpAT that catalyzes the conversion of tryptophan to indole-3-pyruvic acid, an intermediate in auxin biosynthetic pathway. Functional characterization of Arabidopsis the locus tag At4g23600 and At5g36160, annotated as TyrAT, revealed that the enzymes form 4-hydroxyphenylpyruvate from L-Tyr. There are a few reports that plant AAATs converts L-Phe to PPA, but the transamination activity for L-Phe of reported plant AAAT is quite low rather than reaction preferred substrate. Despite substantial efforts for seeking, PheAT has remained unclear. Very recently, a novel PheAT gene in melon was isolated and characterized (*C. melo* AAAT) encoding 45.6 kDa protein and *C. melo* AAAT catalyzed the transamination of L-Phe and L-Tyr to PPA and 4-hydroxyphenylpyruvic acid, respectively. Arabidopsis TyrAT (At5g36160) also formed PPA from L-Phe[41]. Our cloned RyAAAT3 showed high similarity with *C. melo* AAAT at 78% and with Arabidopsis TyrAT (At5g36160) at 74%, whereas RyAAAT3 showed relatively low similarity with Arabidopsis *WEI8/SAV3* (TrpAT) and poppy TyrAT[43] at 50-60%. A phylogenetic tree showed that RyAAATs and some aminotransferases were classified into three clades, AspAT, AlaAT and aminotransferase specific to aromatic amino acid, based on their amino acid sequences (Figure 2-9). Similar to RyAAAT3, *C. melo* AAAT expressed in *E. coli* preferred L-Phe as a substrate by 3.5 fold higher than L-tyrosine. We here propose that the RyAAAT3 and the *C. melo* AAAT are 'phenylalanine aminotransferases' within the AAAT clade as these aminotransferases were only reported to have the preference for L-Phe as a substrate. A Blast search of the plant EST database (TIGR Plant Transcript Assembly BLAST Server, http://plantta.jcvi.org/index.shtml) identified EST clones with homology to RyAAAT3 in various plants such as *Arabidopsis thaliana*, *Medicago truncatula*, *Solanum lycopersicum* (tomato), *Helianthus annuus* (sunflower), *Fragaria vesca* (woodland strawberry), *Malus x domestica* (cultivated apple), *Glycine max* (soybean), *Vitis vinifera* (wine grape), *Coffea canephora* (Coffee robusta), *Gossypium raimondii*, *Solanum tuberosum* (Potato) and *Brassica napus* (oilseed rape). Although these ESTs are

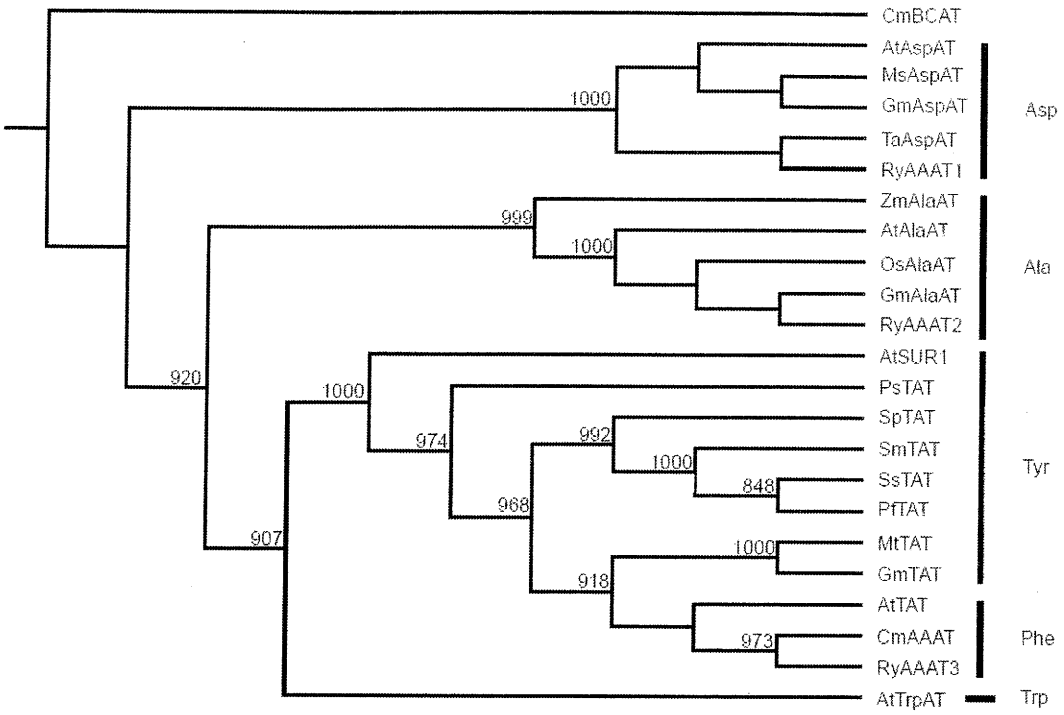

Figure 2-9. A phylogenetic tree of aminotransferases in plant. A phylogenetic tree of members of RyAAATs and AspATs, AlaATs, TrpATs, TyrATs and SUPERROOT 1 are from various plants. The multiple alignments of AAATs performed with ClustalW 1.81. (Abbreviations are as follows: At, *Arabidopsis thaliana*; Cm, *Cucumis melo* L. (melon); Gm, *Glycine max*; Ms, *Medicago sativa*; Mt, *Medicago truncatula*; Os, *Oryza sativa*; Pf, *Perilla frutescens*; Ps, *Papaver somniferum*; Ry, *Rosa* 'Yves Piaget'; Sm, *Salvia miltiorrhiza*; Sp, *Solanum pennellii* (tomato); Ss, *Solenostemon scutellarioides*; Ta, *Triticum aestivum*; Zm, *Zea mays*; BCAT, branched chain aminotransferase; SUR1, SUPERROOT 1 (similar to TyrAT). A molecular phylogenetic tree was constructed by the neighbor-joining (NJ) method. The statistical significance of the NJ tree topology was evaluated by bootstrap analysis 1,000 iterative tree construction. The tree was drawn with CLC Sequence Viewer 6. Bootstrap values (1000 replicates) are given for the nodes. Bootstrap value is shown over 800. All listed aminotransferases are shown Appendix Table 2-2.

annotated as a TyrAT because a PheAT is very new reported, this Blast search findings indicate a possibility of PheAT family would be widely conserved throughout plant kingdom.

In this study, we also have cloned two AAATs (RyAAAT1 and RyAAAT2) besides for RyAAAT3 in rose flower and *in vitro* assay of RyAAAT1 and RyAAAT2 expressed in *E.coli* did not show any transaminase activity toward L-Phe as a substrate (reaction time 10 min, data not shown). A phylogenetic analysis supported this enzymatic result because RyAAAT1 and RyAAAT2 were divided into AspAT and AlaAT clades respectively, not AAAT clade. RyAAAT3 could be originally evolved different from RyAAAT1 and RyAAAT2.

Together, enzymatic findings demonstrated that 2PE is biosynthesized with different pathway in previous reports, tomato, petunia and rose. This study is the first report that rose flowers utilize two different 2PE biosynthetic pathways that L-Phe directly releasing PAld and *via* PPA to produce 2PE from L-Phe. It remains unclear why rose flowers utilize two different 2PE biosynthetic pathways. The transcript patterns of petunia *PAAS* have cyclic ups and downs with daily periodicity, and positively correlated with the production of 2PE in petunia flower[17,44]. It's well known that flower developing synchronize with circadian rhythms and correspond the change of the emission levels of 2PE. Rose AADC may be involved in reproduction process in rose. It reported that the potential biological function of Arabidopsis TyrAT is the defense response to herbivores and pathogens[45,46]. The mRNAs of Arabidopsis TyrAT could be induced by various octadecanoids and by wounding of the plants and accumulation of the Arabidopsis TyrAT protein was observed after application of chemical and physical stresses[47]. Moreover, Song et al (2004) demonstrated that two aminotransferases, AGD2 (At4g33680) and ALD1 (At2g13810) is integral genes in the biosynthesis of phytopathogen resistance chemicals. These findings proposed RyAAAT3 may be an important role in resistance against various environment stresses in rose. Together, rose flower may well manage the regulation of 2PE production related in defense and reproduction.

Appendix Tables

Appendix Table 2-1. Primers list used in Chapter 4. A primer in QuantumRNA Universsal 18S Internal Standard kit (Ambion) was used for 18S rRNA.

Primers	Sequence (5' - 3')
3' RACE PCR	
RyAAAT1	GCITAYCARGGITTYGCIW
RyAAAT2	CTCGGACAGAAGCCTCTAAC
RyAAAT3	CCATGGAGAATGGAACCCATG
5' RACE PCR	
RyAAAT1 for PCR	TGCTCCGGGTTCGATCCTG
RyAAAT1 for nested PCR	TCAAACAGCTGATGTCGCA
RyAAAT2 for PCR	CAGTTCGCAGTTTCTTCCAGG
RyAAAT2 for nested PCR	GTGGAACTGGAACCAGAACC
Full length PCR	
RyAAAT1 Forward	ATGAACTCACTCTCCGCTTCC
RyAAAT1 Reverse	TTAAGCAAGACGAGTAACAGC
RyAAAT2 Forward	CACAGCAATCATGCCACCG
RyAAAT2 Reverse	TTACATCCTTGAATAGCCTCTG
Subcloning to pET28a	
RyAAAT1 Forward (BamH I)	GTGGGATCCATGAACTCACTCTCCGCTTC
RyAAAT1 Reverse (Xho I)	ATACTCGAGAGCAAGACGAGTAACAGCTGC
RyAAAT2 Forward (EcoR I)	GTGGAATTCATGCCACCGAAGGCATTGGAC
RyAAAT2 Reverse (Sal I)	GTGGTCGACCATCCTTGAATAGCCTCTGTC

RyAAAT3 Forward (Sal Ⅰ)	GTGGTCGACGCATGGAGAATGGAACCCATGTG
RyAAAT3 Reverse (Xho Ⅰ)	GCGCTCGAGTAATTTTCTGGCATGCCTTTG
Transcripts analysis	
RyAAAT3 transcripts analysis Forward	CACTGTGGGTCTTCCGCAAAC
RyAAAT3 transcripts analysis Reverse	TCCCAAGGATGCTCGGAACTG
dsRNA synthesis	
RyAAAT3-N terminal T7 promotor	TAATACGACTCACTATAGGGATAAACCCCGGAAATCCTTG
RyAAAT3-N terminal	ATAAACCCCGGAAATCCTTG
RyAAAT3-C terminal T7 promotor	TAATACGACTCACTATAGGGAATGGTTTATCCCCAAAGGC
RyAAAT3-C terminal	AATGGTTTATCCCCAAAGGC

Appendix Table 2-2. The listed aminotransferases in phylogenetic tree.

Aminotransferase	GenBank ID
AtTrpAT	P177213
AtTAT	P200208
GmTAT	AY21813
MtTAT	AY85183
SpTAT1	DZ24702
SmTAT	BC60050
PfTAT	DO17550
SsTAT	AD30341
PsTAT	DC33123
AtSUR1	Q9SIV0
CmAAAT	DC45389
CmBCAT	DC45390
GmAspAT	AC50015
MsAspAT	AA43779
AtAspAT	P196713
TaAspAT	BY58643
GmAlaAT	BW17197
AtAlaAT	P177215
OsAlaAT	AO84040
ZmAlaAT	AAC62456

Chapter Ⅲ

Identification of keto-acid decarboxylase from rose petals

Ⅲ-1. Introduction

We demonstrated that in rose flowers protoplasts PPA was transformed to 2PE. PPA administration increased 2PE amounts in rose protoplasts, implying that rose flowers have KDC, specific to PPA, to yield PAld. However there is no report about Ehrlich pathway and KDC, especially PPA as a substrate, in *planta*. Therefore we purified and decarboxylase towards to PPA in rose flower petals.

Ⅲ-2. Material and methods

Ⅲ-2-1. Purification of the KDC involved in the transformation of PPA to PAld

Flowers at stage 4 to 5 were combined and crushed in liquid nitrogen. This powder (about 100 g) was extracted with 1 L of buffer A (50 mM citrate buffer, pH 6.0, containing 1% polyoxyethylene (10) octylphenyl ether, and Tryton X-100) (Wako Pure Chemicals) in the presence of 100 g PVPP (Polyclar 10, ISP Japan) and stirred for 2 hours at 4 °C. After filtering with gauze, the filtrate was centrifuged (10,000 × *g*, 30 min, 4 °C). The supernatant (crude enzyme extract) was fractionated with ammonium sulfate. Proteins that precipitated in 20% to 60% saturated ammonium sulfate were redissolved in about 40 ml of buffer B (20 mM potassium phosphate buffer, pH 7.5). This fraction was dialyzed in buffer B for 4 hours at 4 °C. The dialysates were further purified by chromatography using a HiTrap DEAE FF column (5 ml, GE Healthcare) equilibrated with buffer C (20 mM potassium phosphate buffer, pH 7.5, containing 1 mM DTT and 1 mM TPP), and eluted with a linear 0–1.5 M NaCl gradient in the same buffer. Ammonium sulfate was added to the eluted fraction to a concentration of 20% and the solution was applied to a HiTrap Phenyl HP column (5 ml, GE Healthcare) equilibrated with buffer D (50 mM potassium phosphate buffer, pH 7.0, containing 1 M ammonium sulfate, 1 mM DTT and 1 mM TPP). The proteins were eluted in buffer D without the ammonium sulfate in a stepwise manner: 20% buffer D for 8 column volumes (CV), 35% buffer D for 5 CV, 50% buffer D for 10 CV, and 100% buffer D for 5 CV. Further purifications were conducted by Superdex 200 14/350 column chromatography (CV 70 ml, GE Healthcare) equilibrated with buffer E (50 mM potassium phosphate buffer, pH 7.0, containing 0.15 M NaCl, 1 mM DTT and 1 mM TPP). The resulting proteins were analyzed by SDS-PAGE (7.5% polyacrylamide gel) and visualized after Ag staining (Nacalai Tesque, Kyoto Japan).

Ⅲ-2-2. Preparation and determination of peptide sequences by Nano-LC-TOF MS

Purified proteins were separated by SDS-PAGE, then the major bands were excised from the gel and destained with wash solution (25 mM NH_4HCO_3/MeCN (1:1 v/v)). Proteins in the gel pieces were reduced and alkylated by treatments with 10 mM dithiothreitol/50 mM NH_4HCO_3 (30 min at 56 °C) and 55 mM iodoacetoamide/50 mM NH_4HCO_3. After sequential washings with wash solution and MeCN, the proteins were digested with trypsin (Sequencing grade modified, Promega) at 37 °C overnight. The tryptic peptides were extracted from the gel pieces with 50% MeCN containing 1% formic acid, and the extracts were pooled and concentrated in a vacuum centrifuge. The dissolved sample was centrifuged at 20,000 *g* for 10 min at room temperature and the supernatant was subject to LC-MS/MS analysis. Peptide assignments were performed using a Nano Frontier eLD system (Hitachi High-Technologies, Tokyo, Japan) based on an LC-ESI-LIT-q-TOF mass spectrometer. The LIT-TOF and CID modes were used for MS detection and peptide fragmentation. The trypsin-treated sample (10 μl) was injected and the peptides trapped on a C18 column, Monolith Trap (50 μm × 150 mm, Hitachi High technologies). Peptide separation was achieved using a packed nano-capillary column (capillary-Ex nano mono cap, 0.05 × 150 mm, GL Science, Japan) at a flow rate of 200 nL/min. The separated peptides were then ionized with a capillary voltage of 1,700 V. The ionized peptides were detected at a detector potential TOF of 1,850 V. The peptides were eluted using a MeCN gradient (A: 2% MeCN containing 0.1% formic acid; B: 98% MeCN containing 0.1% formic acid; 0 min with A = 98%, B = 2% followed by 60 min with A = 60%, B = 40%). All peptide mass data were analyzed using the Peaks software (Bioinformatics Solutions Inc.) and the MASCOT database.

Ⅲ-2-3. Molecular cloning of RyPDC, and expression in insect cells

Degenerate primers were designed based on the rose PDC peptide sequences obtained by *de novo* sequencing performed by Peaks Ver.5.1 and a database search by Mascot. Molecular cloning was conducted using the 3'-RACE and 5'-RACE methods. Heterogeneous expression in HighFive cell (Invitrogen) was performed as described previously[48]. After PBS wash three times, proteins extracted from the transfected cells with 100 mM citrate buffer (pH 6.0) containing 1% TritonX-100 were subjected to SDS-PAGE and PDC activity assays.

Ⅲ-2-4. RyPDC substrate specificity

Substrate specificity for decarboxylation was determined by measuring the various aldehydes as products. For PPA, benzoylformic acid, and 3-indoleglyoxilic acid, the reaction components were as described in the Methods. The reaction was initiated by the addition of the amino acid and performed at 40 °C under Vmax conditions for PPA. The reaction was stopped by adding 400 μl hexane:ethylaccetate (1:1 v/v), 3-phenylpropion aldehyde (Wako Pure Chemicals) as the internal standard, and anhydrous sodium sulfate. Analyses of benzaldehyde and indole-3-carboxyaldehyde were performed using a GC-MS QP2010 Plus (Shimadzu) controlled by the GC Solution (Shimadzu). The GC was equipped with a capillary DB-5ms column (Agilent) of 15m × 0.25 mm I.D. and 0.25 μm film thickness. For benzaldehyde, the column temperature was elevated from 40 °C (3 min hold) to 90 °C (10 °C/min), to 130 °C (30 °C/min), and then to 290 °C (40 °C/min, 3 min hold). For indole-3-carboxyaldehyde, the column temperature was elevated from 70 °C (2 min hold) to 90 °C (10 °C /min), to 130 °C (30 °C/min), and then to 290 °C (40 °C/min, 3 min hold). The injector temperature was 200 °C, the ionizing voltage was 70 eV, and the *m/z* values were as follows: PAld, *m/z* 91 and 120; benzaldehyde, *m/z* 77, 105 and 106; indole-3-carboxyaldehyde, *m/z* 91, 116, 144, and 145. For the analyses of other keto-acids and their esters, the reaction was stopped by adding 400 μl 2,4-DNPH dissolved in ethylacetate, and derivatized at 37 °C for 30 min. After centrifugation, the organic phase was filtered (Millex LH, Millipore) and analyzed by HPLC. The separation module was equipped with a SHIMADZU SPD-20A UV-VIS detector and a CAPSELL PAK C18-UG120 column (2.0 mm × 75 mm, SHISEIDO). The solvents were A: water, and B: MeCN. The column was developed by increasing the latter from 40% to 70% in 15 min, then to 100% with a 5 min hold, at a flow rate of 0.2 ml/min at 40 °C. The wavelengths were 254 and 370 nm. Pyruvate, methylpyruvate, ethylpyruvate, and isoamylpyruvate were dissolved in dimethyl sulfoxide (final concentration 5%) and these solutions were used to confirm that the activities were not different between the aqueous and dimethyl sulfoxide solutions.

Ⅲ-2-5. RNAi suppression experiments

Two kinds of double strand RNA (dsRNA) were prepared based on AADC and PDC partial sequences. The dsRNAs of AADC and PDC were synthesized using the T7 RiboMAX System (Promega) and annealed by incubation at 70 ℃ for 10 min[31,32]. The rose protoplasts (3×10^5 in 200 μL buffer) were transfected with 75 μg dsRNA using a PEG-Ca (200 μL 40% PEG (Fluka)) transfection method[33]. After incubation for 24 h at

30 °C, 2.5 μmol L-[$^2H_8$]Phe was added to the protoplasts and they were incubated for another 24 h at 30 °C. 2PE extraction and GC-MS analysis was carried out as described above. Effect of specific knockdown was confirmed by real-time PCR and described in the Appendix Table 3-1. All knockdown experiments for *AADC*, *PDC* and *AAAT* were conducted under the same conditions.

Ⅲ-3. Results

Ⅲ-3-1. Purification of KDC from the rose flowers

We purified a KDC from rose petal extracts guided by the detection of PAld by GC-MS in the presence of PPA and each of the protein fractions (Table 3-1). In the active fraction, a prominent protein of 60 kDa was detected by SDS-PAGE (Figure 3-1). This band was subjected to trypsin digestion and analyzed by Nano-LC-TOF MS (Table 3-2). The *de novo* sequencing revealed that several of the resultant peptides showed similarity to pyruvate decarboxylase (PDC), which is member of the KDC family.

Ⅲ-3-2. Catalysis of rose RyPDC, decarboxylation of PPA to yield PAld

The full length cDNA of rose PDC was cloned using degenerated primer designed with partial amino acid sequence of rose PDC (Figure 3-2) and the rose PDC was heterogeneously expressed in baculovirus-insect cell system. The rose PDC produced PAld detected at a retention time (4.25 min) that coincided with that of authentic PPA, although PPA was slightly converted to PAld in reaction buffer (Figure 3-3). To investigate the substrate preference of rose PDC, we analyzed relative activity of PDC with various keto-acids and their esters as substrates by GC-MS and HPLC (Figure 3-4). Rose PDC showed the high activity toward pyruvic acid (PA), its esters, and keto-acids with short alkyl chain, whilst keto-acids with aromatic ring, PPA, benzoylformic acid and 3-indoleglyoxylic acid, were poor substrates at rates of less than 1% of the conversion rates of PA and its esters. The rose PDC favors PA as a substrate but catalyzes the transformation of PPA yet at relatively low levels.

Ⅲ-3-3. RNA interference of key enzymes, *AADC* and *RyPDC*, in [$^2H_8$]- and [$^2H_7$]-2PE

To elucidate the contributions of AADC and PDC enzymes to 2PE synthesis in each season, we performed RNAi suppression experiments targeting both enzymes in the rose protoplasts systems. Each double strand RNA (dsRNA) prepared based on *AADC* and *PDC* partial sequence was utilized for RNAi experiments. 2PE production in non-treatment (NT) samples was almost the same to that in control samples (CNT)

Table 3-1. Purification step of the KDC (PDC) involved in PPA metabolism. Steps in the purification of the PDC from a crude extract of *R.* 'Yves Piaget' flowers. Decarboxylation activity was measured by GC-MS with 3-phenylpropion aldehyde (Wako Pure Chemicals) as an internal standard.

Step	Total protein (mg)	Specific Activity (U/mg protein)	Total activity (U)	Purification Fold	Recovery (%)
Crude extracts	739.3	0.91	670.7	1.0	100
Ammonium sulfate	624.5	0.22	137.8	0.2	84
DEAE sepharose	17.2	1.23	21.1	1.4	2.3
Phenyl sepharose	1.88	4.22	7.9	4.7	0.25
Superdex 200 p.g.	0.039	47.24	1.8	52.1	0.005

U : nmol/h

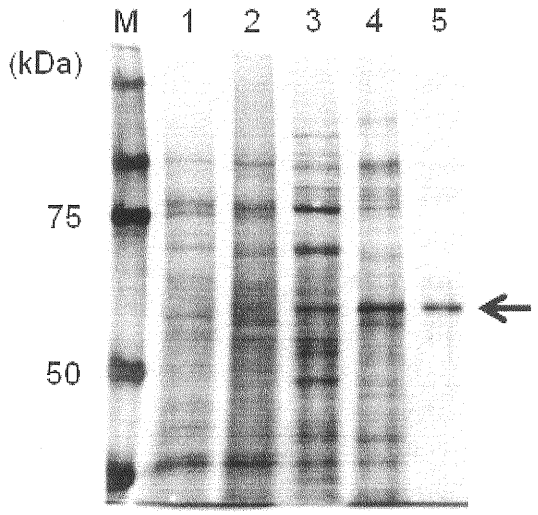

Figure 3-1. SDS-PAGE of KDC (PDC) purification and heterogeneously expressed PDC protein. Gel shows SDS-PAGE of samples obtained from each purification step. The proteins were separated on a 7.5% polyacrylamide gel. M, protein molecular marker purchased from Bio-Rad Ltd. The crude extracts sample, ammonium sulfate precipitates (30%–60%), samples after purification by Hi-Trap DEAE FF, Hi-Trap Phenyl HP and superdex 200 pg. were shown.

Table 3-2. Peptide sequences analyzed LC-MSMS for purified KDC (PDC). Peptide fragments analyzed using the Peaks software Ver.5.1.

Sequence	Ion Score	Charge	Observed *m/z*
AILVQPDR	57.4	2+	456.2814
AVKPVMVGGPK	83.2	1+	1081.632
AVKPVM[2]VGGPK	78	1+	1097.627
DFLLGLAK	54.9	2+	438.7758
ELLEWGSR	40.7	2+	495.2708
IFVPDGHPLK	82.5	1+	1121.623
ILHHTIGLPDFSQELR	99	3+	626.0283
MGLEAAVEAAAEFLNK	97.2	1+	1662.829
M[2]GLEAAVEAAAEFLNK	93.9	2+	560.6279
NWNYTGLVDAIHNGEGK	75.4	3+	629.9933
VNVLFQHIQK	71	3+	409.2527
VRC[1]EEELIEAIETANGPK	63.4	3+	686.6997
VSAANSRPPNPQ	11.6	2+	619.3344
VTIGNGPAFGC[1]VLMK	96.9	2+	782.4313

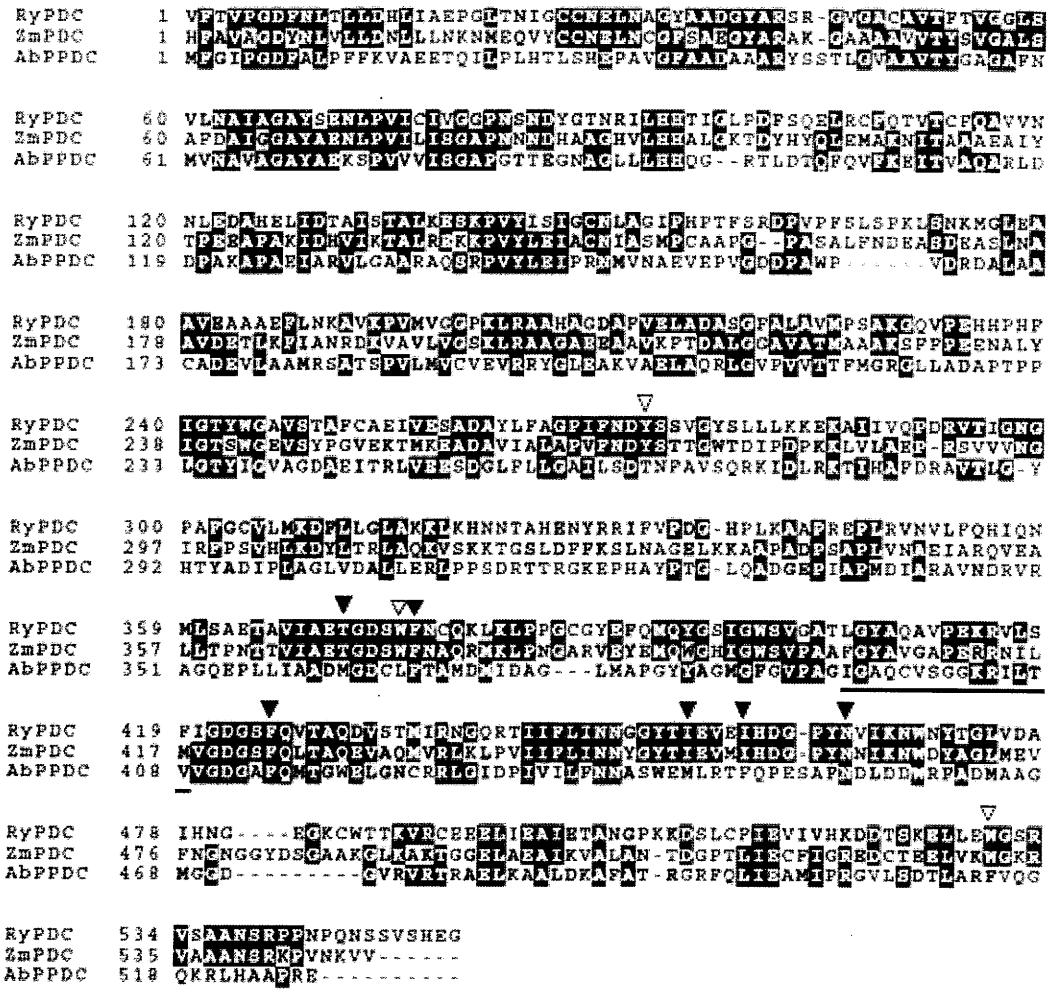

Figure 3-2. Amino acid sequence multiple alignments of RyPDC and bacterial PDC/PPDC. *Zymomonas mobilis* PDC (ZmPDC, Swiss-Prot: P06672) and *Azospirillum brasilense* Phenylpyruvate decarboxylase (AbPPDC, Swiss-Prot: P51852). Black arrowheads indicate key residues forms hydrophobic substrate binding pockets and white arrowheads indicate key residues which determine a cavity volume in substrate binding. Underline shows predicted TPP binding site.

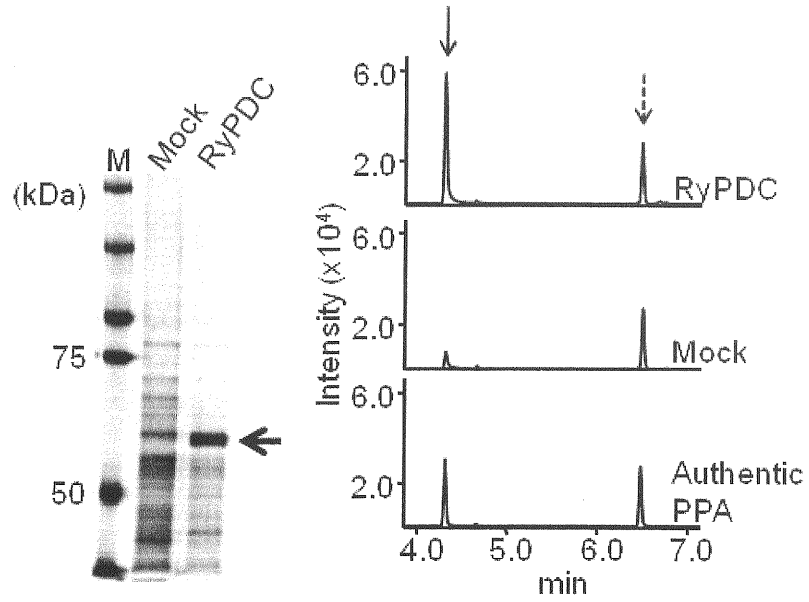

Figure 3-3. Total ion traces on GC-MS analysis of PPA metabolites produced with heterogeneous PDC extracted from insect cells. Only cultures expressing PDC produced PAld (arrows). All chromatograms show the internal standard (dashed arrow).

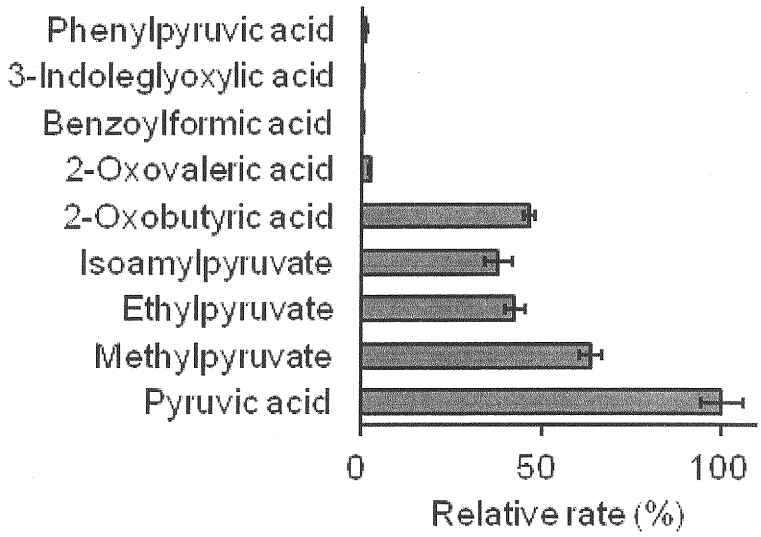

Figure 3-4. Relative conversion rates are shown for selected keto-acids and their esters to their aldehydes, catalyzed by the heterogeneous PDC. Substrate specificity was determined under PPA V_{max} conditions. The activity with PA was set to 100%. Keto-acids and its esters were used at concentration of 5 mM.

(Figure 3-5 *A-D*). The AADC knockdown lines showed drastic decreases in 2PE production in the November to April samples ($P<0.05$), but only slight decreases in the May to October samples as compared with the control (Figure 3-5 *A* and *B*). On the other hand, the PDC knockdown lines showed slight decreases in 2PE production in the November to April samples and a decrease of about 50% in the May to October samples ($P<0.01$) as compared with the control (Figure 3-5 *C* and *D*). These results supported that the rose PDC functions in the novel 2PE biosynthetic pathway from May to October, but does not contribute to 2PE synthesis from November to April.

Ⅲ-4. Discussion

In KDC family, phenylpyruvate decarboxylase (PPDC) catalyzes the decarboxylation of PPA. PPDC however have not been reported in plants. We purified a rose PDC showing a decarboxylation activity toward PPA. Based on the partial sequences its gene was identified and the enzyme it encodes was functionally characterized. Rose PDC is the first instance of a plant PDC showing PPA decarboxylation activity. Rose PDC (RyPDC) is a 605 amino acid protein with a calculated average molecular weight of 65,038 Da and pI of 5.75, and includes a TPP binding site (LGYAQAVPEKRVLSF). The deduced amino acid sequences of RyPDC showed 97% similarity to *Fragaria x ananassa* PDC (GenBank: AAG13131) and distinguished from other KDCs, PPDC and indole pyruvate decarboxylase (IPDC), in amino acid sequence (Fig. 3-6). Recombinant RyPDC produced PAld from L-Phe enzymatically, although it is proposed that in microorganisms PPA decarboxylation is catalyzed by PPDC and PDC is not preferred due to their bulky amino acid residues (*e.g.* Trp and Tyr) around the active site pocket[49,50]. However in *Enterobacter cloacae* IPDC, an active site pocket is substantially larger as predicted from amino acid residues because of a rotation of one dimer towards the other[51]. RyPDC forms tetramer, dimer of dimer, similar to other PDCs[51,52] (Fig. 3-7) and some residues at predicted tetramer interface is diversified among microorganism and plant PDC. Thus dimer rotation except active site pocket might contribute to PPA catalysis of RyPDC. PDC is found in *planta* and known as an enzyme catalyzing PA decarboxylation for ethanol fermentation. *Arabidopsis thaliana PDC1* null mutant decreased acetaldehyde production[53]. Similarly heterozygous petunia *PDC2* mutant was essentially inactive in acetaldehyde production. Also, PDC in cottonwood leaf vein should contribute to acetaldehyde production[54]. Since PDC is extensively conserved in plant, it is possible that other plant might produce 2PE by AAAT-PDC route.

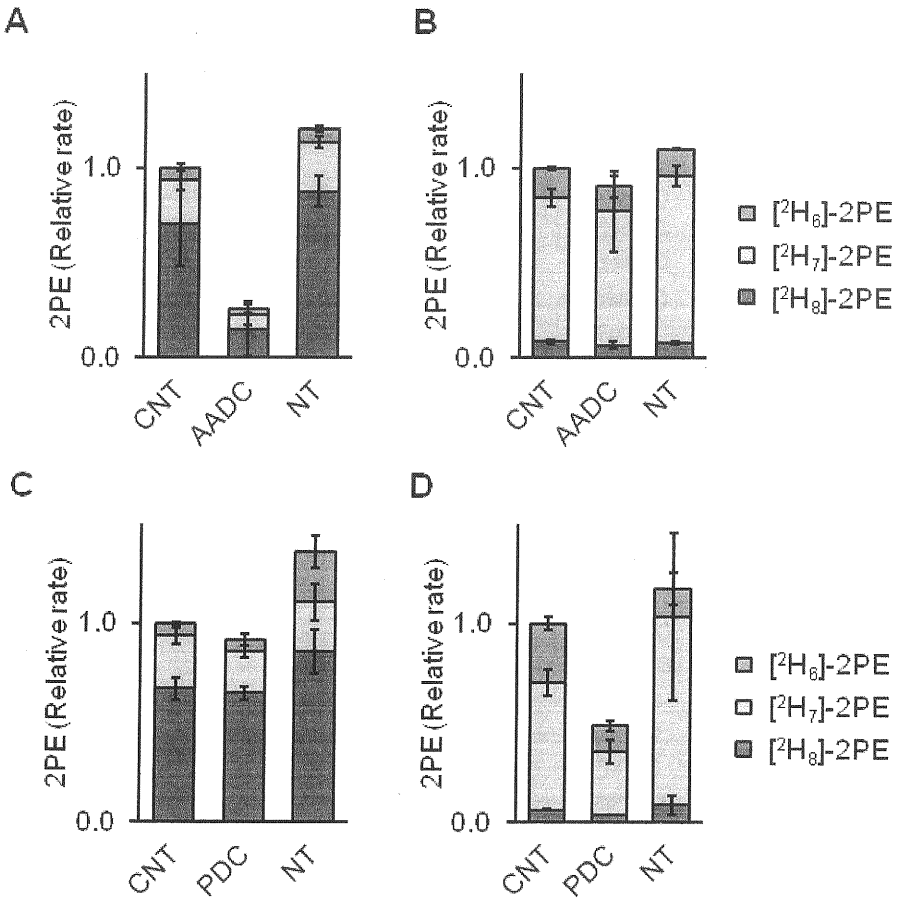

Figure 3-5. Effects of RNAi-mediated silencing of the *AADC* and *PDC* genes. [^2H_n, n=6–8]-2PE synthesis was measured in protoplasts prepared from rose petals harvested between November and April (A, C) and between May and October (B, D). The protoplasts (3×10^5 cells) were transfected with dsRNA designed to knockdown *AADC* (A, B) and *PDC* (C, D) respectively. The control (CNT) and knockdown groups were treated with PEG-Ca solution, and the NT groups were not treated.

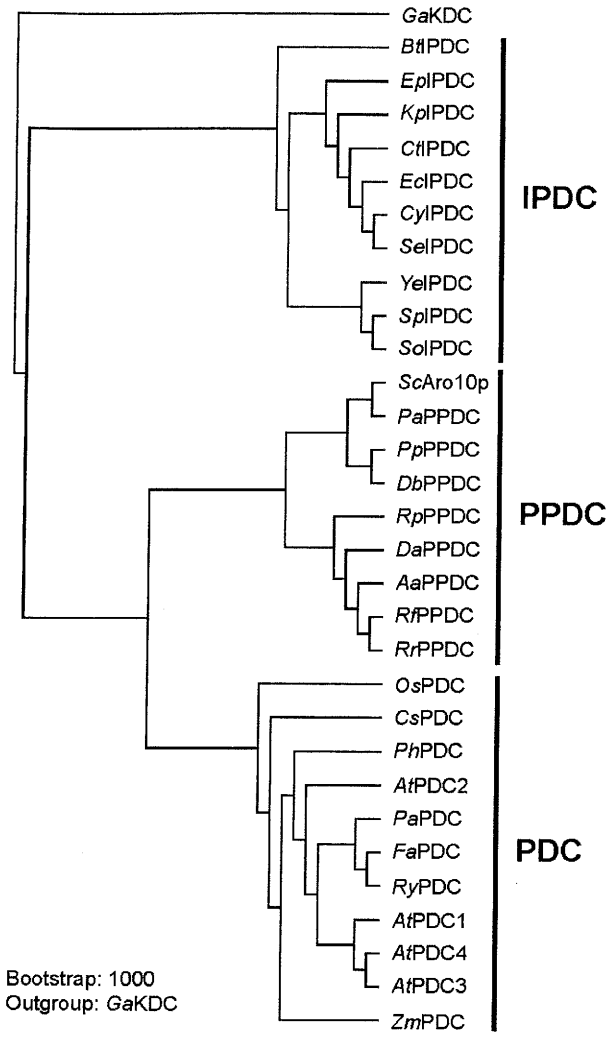

Figure 3-6. A phylogenetic tree of PDC proteins and KDC proteins, PPDC and IPDC. A phylogenetic tree of KDC members. The multiple alignment of members of the decarboxylase exhibiting high similarity to rose PDC from various plants was constructed with ClustalW 1.81. Abbreviations are as Appendix Table. *Ga*KDC was included in the alignment as an outgroup. Based on the alignment, a molecular phylogenetic tree was constructed by the neighbor-joining (NJ) method. The statistical significance of the NJ tree topology was evaluated by bootstrap analysis 1,000 iterative tree construction. The tree was drawn with Tree Viewer Version 1.6.6.

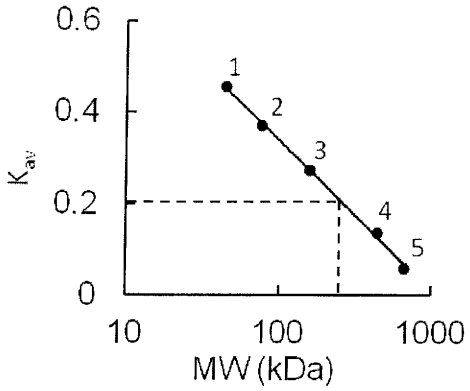

No.	Protein	Molecular weight (kDa)
1	Thyroglobulin	669
2	Ferritin	440
3	Aldolase	158
4	Conalbumin	75
5	Ovalbumin	44

Figure 3-7. Determination of PDC molecular weight. Native PDC protein extracted from rose petals was calculated as 255 kDa by gel filtration. Standard curve was drawn by Gel Filtration Standard (Bio-Rad).

Appendix Tables

Appendix Table 3-1. Primers list used in Chapter 3

Primers	Sequence (5' - 3')
3' RACE	
RyPDC	GCIATHCAYAAYGGIGARGG
5' RACE	
RyPDC for PCR	GGTGGGCGGCTGTTGGCAGCAGAAACCC
Full length	
RyPDC, Forward	GTTTCAATCTTTAGACCTCC
RyPDC, Reverse	GGCATTCATGTGATACAGAAGAG
Subcloning to pFast Bac	
RyPDC, Forward (HindⅢ)	GCGAAGCTTATGGACACCAAGATTGGCTC
RyPDC, Reverse (Xho Ⅰ)	ATACTCGAGCTGAGGATTAGGTGGGCGGC
dsRNA preparation	
RyAADC-N terminal T7 promotor	TAATACGACTCACTATAGGGTTCATTAACGGCGTAGAGGG
RyAADC-C terminal	AAGGCAACAGCAATCCATTC
RyAADC-N terminal	TTCATTAACGGCGTAGAGGG
RyAADC-C terminal T7 promotor	TAATACGACTCACTATAGGGAAGGCAACAGCAATCCATTC
RyPDC-N terminal T7 promotor	TAATACGACTCACTATAGGGAGGAACATACTGGGGTGCTG
RyPDC-C terminal	GAGCGAGTACCCAACAGAGC
RyPDC-N terminal	AGGAACATACTGGGGTGCTG
RyPDC-C terminal T7 promotor	TAATACGACTCACTATAGGGGAGCGAGTACCCAACAGAGC
qRT-PCR	
RyAADC, Forward	ATGGGAGTACTTGTGAGGCCAT
RyAADC, Reverse	CCCAAATTCTCGCTACCAATTC
PDC, Forward	TGCAGTTGAGGCAGCGGCAG
PDC, Reverse	GCATGTGCAGCGCGCAGTTT
RyAAAT, Forward	TGAAGGTTGCAGGACCGCCC
RyAAAT, Reverse	TGGATGGCGGCTTGGTTGGT
Ryβ-Actin, Forward	CTGAGGCTCCTCTTAACCCC
Ryβ-Actin, Reverse	CATACATAGCGGGCACATTG

Appendix Table 3-2. The listed keto-acid decarboxylase families in phylogenetic tree.

Keto-acid decarboxylase	GenBank ID
GaKDC	ZP08317680
ScARO10P	Q06408
AaPPDC	YP160767
RfPPDC	ABD68270
RrPPDC	YP427803
RpPPDC	ABD07130
PpPPDC	XP002493734
DbPPDC	AEH16575
DaPPDC	YP388823
EclPDC	P23234 [UniProt]
CylPDC	ZP06351948
SelPDC	ZP03220347
CtlPDC	YP003211360
KplPDC	YP002237253
EplPDC	YP002648186
SpPlPDC	AEL12170
SolPDC	ZP06639356
YelPDC	YP001005545
BtlPDC	ADY21754
FaPDC	AAL37492
PhPDC	AAX33299
PaPDC	ABZ79223
ZmPDC	AAL99745
RyPDC	AB669188
OsPDC	AAA68290
AtPDC4	AT5G01320
AtPDC3	AT5G01330
AtPDC1	AT4G33070
AtPDC2	AT5G54960

Chapter Ⅲ

Summary

Summary

2-Phenylethanol (2PE) is one of the prominent scent compounds produced by Damask roses such as *Rosa x damascena*, *R.* 'Hoh-Jun', and *R.* 'Yves Piaget'. There is considerable interest in elucidating the biosynthetic pathways of 2PE, especially in rose flowers where it is a predominant volatile.

A pulse chase feeding experiment of deuterium labeled L-phenylalanine (L-[$^2H_8$]Phe) to rose flowers reveals that [$^2H_8$]-2PE is biosynthesized without loss of a-deuterium from L-[$^2H_8$]Phe by the action of two enzymes, pyridoxal phosphate (PLP)-dependent aromatic amino acid decarboxylase (AADC) and phenylacetaldehyde reductase (PAR). We previously developed a simple and controllable approach to elucidate the biosynthesis of 2PE in rose using the isolated protoplasts of rose flowers (Yang et al. 2009). In this experimental model, L-[$^2H_8$]Phe administration to protoplasts resulted in [$^2H_7$]-2PE production at some point, implying that [$^2H_7$]-2PE was biosynthesized in different route from well known route (AADC-PAR route). Therefore we in this study we designed experiments to elucidate the alterative biosynthetic pathway to 2PE.

In Chapter I, we describe the production of [^2H_n, n=6-8]-2PE isotopologues. Over a couple of years in Shizuoka, Japan, we conducted L-[$^2H_8$]Phe feeding experiments with protoplasts made from flowers of *R.* 'Yves Piaget'. We found that [$^2H_7$]-2PE (*m/z* 129 $[M]^+$) as the main product ([$^2H_8$]/[$^2H_7$]/[$^2H_6$]-2PE=9.8/76.4/13.9) was detected in the protoplasts collected in summer (August, 2008) whereas [$^2H_8$]-2PE (*m/z* 130 $[M]^+$) became the dominant product ([$^2H_8$]/[$^2H_7$]/[$^2H_6$]-2PE=75.6/21.0/3.4) in winter (January, 2009). Based on the results, [$^2H_7$]-2PE was dominantly produced with a loss of ^2H at a-position (C-2) of L-[$^2H_8$]Phe in summer season. These results led us a hypothesis that the new 2PE biosynthetic pathway includes the intermediate phenylpyruvic acid (PPA) and two key enzymes: aromatic amino acid aminotransferase (AAAT) and keto-acid decarboxylase (KDC). Furthermore, we administered L-[$^2H_8$]Phe to the floral protoplasts harvested once every month from May 2009 to July 2010. [$^2H_7$]-2PE was the dominant species detected among the [^2H_n, n=6–8]-2PE isotopologues from May to October although low levels of [$^2H_8$]-2PE were also detected. In contrast, [$^2H_8$]-2PE was the dominant compound detected from November to April. Also, [$^2H_8$]-2PE was synthesized constantly throughout the year and [$^2H_7$]-2PE was synthesized with 5–10 fold higher than the [$^2H_8$]-2PE from May to October. Thus this seasonal pathway to [$^2H_7$]-2PE was activated in May-October samples.

To confirm the involvement of PPA, a key intermediate, in the new 2PE biosynthesis, we determined L-[$^2H_8$]Phe transformation to [$^2H_7$]PPA in rose protoplasts. Also, during the May-October, [^2H_n, n=6-7]PPA and 2PE synthesis from L-[$^2H_8$]Phe and PPA respectively in protoplasts were significantly higher than the November-April, suggesting that the hypothetical biosynthetic route *via* PPA contributed to the seasonal pathway to 2PE.

In Chapter II, we obtained and functionally characterized rose AAAT (RyAAAT). Blast searching and degenerate PCR cloning from rose petals gave us full length cDNA of RyAAAT. *E. coli* expressed enzymes and showed PPA production activity with L-Phe. The deduced amino acid sequences of RyAAAT3 showed 78% similarity to *Cucumis melo* L. AAAT. Furthermore RyAAAT3 gave the highest transaminase activity with L-Phe as a substrate among several amino acids such as D-phenylalanine, L-tyrosine, L-tryptophan, L-alanine and glycine. To elucidate the contributions of *RyAAAT3* to 2PE synthesis in the rose flowers, we performed RNAi experiments targeting *RyAAAT3* in the rose protoplasts. 2PE production in non-treated samples was almost the same compared to control samples. RNAi experiments towards *RyAAAT3* decreased 2PE production at about 60% as compared with the control samples. These results suggested *RyAAAT3* plays an important role in 2PE biosynthesis of in rose flowers.

In Chapter III, to identify the KDC, we purified a KDC from rose petal extracts guided by the detection of PAld by GC-MS in the presence of PPA. In the active fraction, a prominent protein of approximately 60 kDa was detected by SDS-PAGE. This band was identified pyruvate decarboxylase (PDC), which is member of the KDC family by LC-MSMS analysis. The full length cDNA of rose PDC (RyPDC) was cloned and heterogeneously expressed in baculovirus-insect cell system. The RyPDC showed the high activity toward pyruvic acid, whilst PPA was poor substrates at rates of less than 1% of the conversion rates of PA and its esters. The RyPDC favors pyruvic acid as a substrate but catalyzes the transformation of PPA yet at relatively low levels. To elucidate the contributions of RyPDC to 2PE synthesis in each season, we performed RNAi experiments in the rose protoplasts systems. The RyPDC knockdown lines showed slight decreases in 2PE production in the November to April samples and a decrease of about 50% in the May to October samples ($P<0.01$) as compared with the control. These results supported that the rose PDC functions in the new 2PE biosynthetic pathway from May to October, but does not contribute to 2PE synthesis from November to April.

Acknowledgements

We thank Drs. S. Baldermann, V. K. Deo, Z.Y. Yang for informative discussion and critical reading of this manuscript. We also thank Ichikawa Rosary for supplying the roses throughout our study and Ms. Y. Ryuno for technical support. The work is supported in part by the Grand-in-Aid for Scientific Research (B), JSPS to N.W.

References

1. Pichersky E, Noel JP, Dudareva N. Biosynthesis of plant volatiles: nature's diversity and ingenuity. Science 2006;311:808-11.

2. Jetter R. Examination of the processes involved in the emission of scent volatiles from flowers. Biology of Floral Scent 2006:125–143.

3. Barfod AS, Hagen M, Borchsenius F.Twenty-five years of progress in understanding pollination mechanisms in palms (Arecaceae). Ann Bot. 2011;108:1503-16.

4. Raguso AR and Pichersky E. Floral volatiles from Clarkia breweri and C. concinna (Onagraceae) recent evolution of floral scent and moth pollination. Plant Syst. Evol. 1995;194:55–67.

5. Negre F, Kish CM, Boatright J, Underwood B, Shibuya K, Wagner C, Clark DG, Dudareva N. Regulation of methylbenzoate emission after pollination in snapdragon and petunia flowers. Plant Cell. 2003;15:2992-3006.

6. Aubert C, Baumann S, Arguel H. Optimization of the analysis of flavor volatile compounds by liquid-liquid microextraction (LLME). Application to the aroma analysis of melons, peaches, grapes, strawberries, and tomatoes. J Agric Food Chem. 2005;53:8881-95.

7. Marilley L, Casey MG. Flavours of cheese products: metabolic pathways, analytical tools and identification of producing strains. Int J Food Microbiol. 2004;90:139-59.

8. Schwab W, Davidovich-Rikanati R, Lewinsohn E. Biosynthesis of plant-derived flavor compounds. Plant J. 2008;54:712-32.

9. Hua D, Xu P. Recent advances in biotechnological production of 2-phenylethanol. Biotechnol Adv. 2011;29:654-60.

10. Dudareva N, Andersson S, Orlova I, Gatto N, Reichelt M, Rhodes D, Boland W, Gershenzon J. The nonmevalonate pathway supports both monoterpene and sesquiterpene formation in snapdragon flowers. Proc Natl Acad Sci U S A. 2005;102:933-8.

11. Picone JM, Clery RA, Watanabe N, MacTavish HS, Turnbull CG. Rhythmic emission of floral volatiles from Rosa damascena semperflorens cv. 'Quatre Saisons'. Planta. 2004;219(3):468-78.

12. Hayashi S, Yagi K, Ishikawa T, Kawasaki M, Asai T,Picone J, Turnbull C, Hiratake J, Sakata K, Takada M, Ogawa K and WATANABE N. Emission of 2-phenylethanol from its □-D-glucopyranoside and the biogenesis of these compounds from [2H8] L-phenylalanine in rose flowers. Tetrahedron 2004;60:7005-7013.

13. Theis N. Fragrance of Canada thistle (Cirsium arvense) attracts both floral herbivores and pollinators. J Chem Ecol. 2006;32:917-27.

14. Jürgens A, Webber AC, Gottsberger G. Floral scent compounds of Amazonian Annonaceae species pollinated by small beetles and thrips. Phytochemistry. 2000;55:551-8.

15. Wittstock U, Halkier BA. Cytochrome P450 CYP79A2 from Arabidopsis thaliana L. Catalyzes the conversion of L-phenylalanine to phenylacetaldoxime in the biosynthesis of benzylglucosinolate. J Biol Chem. 2000;275:14659-66.

16. Sakai M, Hirata H, Sayama H, Sekiguchi K, Itano H, Asai T, Dohra H, Hara M, Watanabe N. Production of 2-phenylethanol in roses as the dominant floral scent compound from L-phenylalanine by two key enzymes, a PLP-dependent decarboxylase and a phenylacetaldehyde reductase. Biosci Biotechnol Biochem. 2007;71:2408-19.

17. Kaminaga Y, Schnepp J, Peel G, Kish CM, Ben-Nissan G, Weiss D, Orlova I, Lavie O, Rhodes D, Wood K, Porterfield DM, Cooper AJ, Schloss JV, Pichersky E, Vainstein A, Dudareva N. Plant phenylacetaldehyde synthase is a bifunctional homotetrameric enzyme that catalyzes phenylalanine decarboxylation and oxidation. J Biol Chem. 2006;281:23357-66.

18. Tieman D, Taylor M, Schauer N, Fernie AR, Hanson AD, Klee HJ. Tomato aromatic amino acid decarboxylases participate in synthesis of the flavor volatiles 2-phenylethanol and 2-phenylacetaldehyde. Proc Natl Acad Sci U S A. 2006;103:8287-92.

19. Chen XM, Kobayashi H, Sakai M, Hirata H, Asai T, Ohnishi T, Baldermann S, Watanabe N. Functional characterization of rose phenylacetaldehyde reductase (PAR), an enzyme involved in the biosynthesis of the scent compound 2-phenylethanol. J Plant Physiol. 2011;168:88-95.

20. Tieman DM, Loucas HM, Kim JY, Clark DG, Klee HJ. Tomato phenylacetaldehyde reductases catalyze the last step in the synthesis of the aroma volatile 2-phenylethanol. Phytochemistry. 2007;68:2660-9.

21. Yang Z, Sakai M, Sayama H, Shimeno T, Yamaguchi K, Watanabe N. Elucidation of the biochemical pathway of 2-phenylethanol from shikimic acid using isolated protoplasts of rose flowers. J Plant Physiol. 2009;166:887-91.

22. Ehrlich F. Über die bedingungen der fuselölbildung und über ihren zusammenhang mit dem eiweißaufbau der Hefe. Berichte der Deutschen Chemischen Gesellschaft 1907;40:1027-47.

23. Marilley L, Casey MG. Flavours of cheese products: metabolic pathways, analytical tools and identification of producing strains. Int J Food Microbiol. 2004;90:139-59.

24. Dorman DC, Struve MF, Norris A, Higgins AJ. Metabolomic analyses of body fluids after subchronic manganese inhalation in rhesus monkeys. Toxicol Sci. 2008;106:46-54.

25. Sciacovelli O, Dell'Atti A, DeGiglio A, Cassidei L. Studies on phenylpyruvic acid. I. Keto-enol tautomerism. Z Naturforsch C. 1976;31:5-11.

26. Carpy AJM,Haasbroek PP,Ouhabi J, Oliver DW. Keto/enol tautomerism in phenylpyruvic acids: structure of the o-nitrophenylpyruvic acid. J Mol Struct.2000;520:191-198.

27. Maeda H, Shasany AK, Schnepp J, Orlova I, Taguchi G, Cooper BR, Rhodes D, Pichersky E, Dudareva N. RNAi suppression of Arogenate Dehydratase1 reveals that phenylalanine is synthesized predominantly via the arogenate pathway in petunia petals. Plant Cell. 2010 ;22:832-49.

28. Guterman I, Shalit M, Menda N, Piestun D, Dafny-Yelin M, Shalev G, Bar E, Davydov O, Ovadis M, Emanuel M, Wang J, Adam Z, Pichersky E, Lewinsohn E,

Zamir D, Vainstein A, Weiss D. Rose scent: genomics approach to discovering novel floral fragrance-related genes. Plant Cell. 2002;14:2325-38.

29. Han Q, Ding H, Robinson H, Christensen BM, Li J. Crystal structure and substrate specificity of Drosophila 3,4-dihydroxyphenylalanine decarboxylase. PLoS One. 2010;5:e8826.

30. Bertoldi M, Gonsalvi M, Contestabile R, Voltattorni CB. Mutation of tyrosine 332 to phenylalanine converts dopa decarboxylase into a decarboxylation-dependent oxidative deaminase. J Biol Chem. 2002;277:36357-62.

31. An CI, Sawada A, Fukusaki E, Kobayashi A. A transient RNA interference assay system using Arabidopsis protoplasts. Biosci Biotechnol Biochem. 2003;67:2674-7.

32. An CI, Sawada A, Kawaguchi Y, Fukusaki E, Kobayashi A. Transient RNAi induction against endogenous genes in Arabidopsis protoplasts using in vitro-prepared double-stranded RNA. Biosci Biotechnol Biochem. 2005;69:415-8.

33. Sheen J. Signal transduction in maize and Arabidopsis mesophyll protoplasts. Plant Physiol. 2001;127:1466-75.

34. Huang B, Yi B, Duan Y, Sun L, Yu X, Guo J, Chen W. Characterization and expression profiling of tyrosine aminotransferase gene from Salvia miltiorrhiza (Dan-shen) in rosmarinic acid biosynthesis pathway. Mol Biol Rep. 2008;35:601-12.

35. Yennawar N, Dunbar J, Conway M, Hutson S, Farber G. The structure of human mitochondrial branched-chain aminotransferase. Acta Crystallogr D Biol Crystallogr. 2001;57:506-15.

36. Blankenfeldt W, Nowicki C, Montemartini-Kalisz M, Kalisz HM, Hecht HJ. Crystal structure of Trypanosoma cruzi tyrosine aminotransferase: substrate specificity is influenced by cofactor binding mode. Protein Sci. 1999;8:2406-17.

37. Maeda H, Yoo H, Dudareva N. Prephenate aminotransferase directs plant phenylalanine biosynthesis via arogenate. Nat Chem Biol. 2011;7:19-21.

38. Gonda I, Bar E, Portnoy V, Lev S, Burger J, Schaffer AA, Tadmor Y, Gepstein S, Giovannoni JJ, Katzir N, Lewinsohn E. Branched-chain and aromatic amino acid

catabolism into aroma volatiles in Cucumis melo L. fruit. J Exp Bot. 2010;61:1111-23.

39. Lopukhina A, Dettenberg M, Weiler EW, Holländer-Czytko H. Cloning and characterization of a coronatine-regulated tyrosine aminotransferase from Arabidopsis. Plant Physiol. 2001 ;126:1678-87.

40. Stepanova AN, Robertson-Hoyt J, Yun J, Benavente LM, Xie DY, Dolezal K, Schlereth A, Jürgens G, Alonso JM. TAA1-mediated auxin biosynthesis is essential for hormone crosstalk and plant development. Cell. 2008;133:177-91.

41. Tao Y, Ferrer JL, Ljung K, Pojer F, Hong F, Long JA, Li L, Moreno JE, Bowman ME, Ivans LJ, Cheng Y, Lim J, Zhao Y, Ballaré CL, Sandberg G, Noel JP, Chory J. Rapid synthesis of auxin via a new tryptophan-dependent pathway is required for shade avoidance in plants. Cell. 2008 ;133:164-76.

42. Prabhu PR, Hudson AO. Identification and Partial Characterization of an L-Tyrosine Aminotransferase (TAT) from Arabidopsis thaliana. Biochem Res Int.

43. 2010;2010:549572.

44. Lee EJ, Facchini PJ. Tyrosine aminotransferase contributes to benzylisoquinoline alkaloid biosynthesis in opium poppy. Plant Physiol. 2011;157:1067-78.

45. Farhi M, Lavie O, Masci T, Hendel-Rahmanim K, Weiss D, Abeliovich H, Vainstein A. Identification of rose phenylacetaldehyde synthase by functional complementation in yeast. Plant Mol Biol. 2010;72:235-45

46. Song JT, Lu H, Greenberg JT. Divergent roles in Arabidopsis thaliana development and defense of two homologous genes, aberrant growth and death2 and AGD2-LIKE DEFENSE RESPONSE PROTEIN1, encoding novel aminotransferases. Plant Cell. 2004;16:353-66.

47. Song JT, Lu H, McDowell JM, Greenberg JT. A key role for ALD1 in activation of local and systemic defenses in Arabidopsis. Plant J. 2004;40:200-12.

48. Lopukhina A, Dettenberg M, Weiler EW, Holländer-Czytko H. Cloning and characterization of a coronatine-regulated tyrosine aminotransferase from Arabidopsis. Plant Physiol. 2001;126:1678-87.

49. Ohnishi T, Watanabe B, Sakata K, Mizutani M. CYP724B2 and CYP90B3 function in the early C-22 hydroxylation steps of brassinosteroid biosynthetic pathway in tomato. Biosci Biotechnol Biochem. 2006;70:2071-80.

50. Versées W, Spaepen S, Vanderleyden J, Steyaert J. The crystal structure of phenylpyruvate decarboxylase from Azospirillum brasilense at 1.5 A resolution. Implications for its catalytic and regulatory mechanism. FEBS J. 2007;274:2363-75.

51. Kneen MM, Stan R, Yep A, Tyler RP, Saehuan C, McLeish MJ. Characterization of a thiamin diphosphate-dependent phenylpyruvate decarboxylase from Saccharomyces cerevisiae. FEBS J. 2011;278:1842-53.

52. Schütz A, Sandalova T, Ricagno S, Hübner G, König S, Schneider G. Crystal structure of thiamindiphosphate-dependent indolepyruvate decarboxylase from Enterobacter cloacae, an enzyme involved in the biosynthesis of the plant hormone indole-3-acetic acid. Eur J Biochem. 2003;270:2312-21.

53. Furey W, Arjunan P, Chen L, Sax M, Guo F, Jordan F. Structure-function relationships and flexible tetramer assembly in pyruvate decarboxylase revealed by analysis of crystal structures. Biochim Biophys Acta. 1998;1385:253-70.

54. Kürsteiner O, Dupuis I, Kuhlemeier C. The pyruvate decarboxylase1 gene of Arabidopsis is required during anoxia but not other environmental stresses. Plant Physiol. 2003;132:968-78.

55. Nguyen T, Drotar AM, Monson RK, Fall R. A high affinity pyruvate decarboxylase is present in cottonwood leaf veins and petioles: a second source of leaf acetaldehyde emission? Phytochemistry. 2009;70:1217-21.

Appendix

Summary in Japanese

要約

2-Phenylethanol (2PE) は *Rosa x damascena*、*R.* 'Hoh-Jun'、*R.* 'Yves Piaget' などのダマスク系バラにおける主要かつ特徴的な香気成分である。その香気としての重要性から、2PE 生合成経路には多くの関心が寄せられている。

L-[$^2H_8$]phenylalanine (L-[$^2H_8$]Phe) を用いた無傷植物への投与実験から、我々はこれまでに、2PE がその α 位の重水素を保持したまま [$^2H_8$]-2PE として PLP 依存性の芳香族脱炭酸酵素（AADC）と中間体である phenylacetaldehyde 還元酵素（PAR）の２つの酵素によって生合成されることを明らかにした。我々は新たな簡易的実験モデルとしてバラ花弁から調製したプロトプラストを用いた実験系を確立した（Yang et al., 2009)。この実験系において L-[$^2H_8$]Phe の投与はある時期に [$^2H_7$]-2PE の生成をもたらした。このことから [$^2H_7$]-2PE は既知の生合成経路（AADC-PA R 経路）とは異なる経路で生合成されていることが考えられた。そこで、この研究ではそのもう１つの 2PE 生合成系を解明することを目的とした。

第一章では、重水素化 2PE アイソトポローグの生成に論述した。L-[$^2H_8$]Phe のプロトプラストへの投与実験を複数年繰り返し行ったところ、我々は 8 月に [$^2H_7$]-2PE (*m/z* 129 $[M]^+$) が主要に生成されることを確認した。一方、1 月には [$^2H_8$]-2PE (*m/z* 130 $[M]^+$) が主要な生成物として検出された。この結果から、[$^2H_7$]-2PE は α 位の重水素を保持せずに生合成されることが示唆されたため、我々は phenylpyruvic acid (PPA) を中間体とし、芳香族アミノ基転移酵素（AAAT）とケト酸脱炭酸酵素（KDC）が関与する新規の 2PE 生合成経路を想定した。さらに、この投与実験を月毎に通年実施したところ、5 月から 10 月の時期（夏期）には [$^2H_7$]-2PE が、11 月から 4 月（冬期）には [$^2H_8$]-2PE が主要なアイソトポローグとして検出された。また、[$^2H_8$]-2PE の生成は通年ほとんど一定であるのに対して、[$^2H_7$]-2PE の生成は 11 月から 4 月の間に比べて 5 月から 10 月の間には 5-10 倍量生成されていた。このように [$^2H_7$]-2PE の生合成は夏期に活性化されることが示唆された。

新規の 2PE 経路において PPA を介することを確認するため、L-[$^2H_8$]Phe 投与時のプロトプラストから [$^2H_7$]PPA の生成を確認した。また、プロトプラストに L-[$^2H_8$]Phe、PPA を投与したところ、生成物である [$^2H_7$]PPA、2PE 量は冬期に比べて夏期には有意に増加していた。これらの結果は新規経路において PPA を介して 2PE が生合成されること、また PPA が 2PE 生成の夏期における亢進に寄与していることを示唆するものである。

第二章では、AAAT の機能解明について論述した。バラ花弁から縮重プライマーを用いてクローニングしたバラ AAAT（RyAAAT）候補を大腸菌で発現させたところ、メロン AAAT に高い類似性を示す RyAAAT3 が PPA 生成活性を示した。さらに、RyAAAT3 は芳香族アミノ酸の中で L-Phe に対して最も高いアミノ基転移活性を示した。この RyAAAT3 遺伝子の 2PE 生成への寄与を調べるため、RyAAAT3 遺伝子を RNAi によってノックダウンさせたところ、2PE 生成量は有意に低下した。このことから、RyAAAT3 がバラにおいて 2PE 生成に寄与していることが示唆された。

第三章では、KDC の同定、機能解明について論述した。バラ花弁より PPA への脱炭酸活性を指標として酵素を精製したところ、60 kDa 付近に主要なバンドが確認された。これを LC-MSMS 解析に供したところ、KDC ファミリーの１つであるピルビン酸脱炭酸酵素（PDC）と同定された。このペプチド配列を基にしてバラ PDC (RyPDC) をクローニングし、昆虫細胞を用いて異種発現した。RyPDC はピルビン酸に高い活性を示すものの、PPA を基質として phenylacetaldehyde (PAld) を生成した。RyPDC の 2PE 生成への寄与を RNAi によって調べたところ、RyPDC をノックダウンさせたプロトプラストでは 2PE 生成量が有意に低下した。また、この低下は夏期にのみ確認され、冬期には 2PE 生成量は変化しなかった。これらの結果から、RyPDC は 2PE 新規生合成経路において PPA の脱炭酸を担っており、夏期における 2PE 生成の亢進が新規生合成経路によるものであると示唆された。